

Lepton polarization and CP -violating effects in the $\bar{B} \rightarrow \bar{K}_0^*(1430)\ell^+\ell^-$ decay in the standard and the two Higgs doublet model

F. Falahati,^{*} S. M. Zebarjad, and S. Naeimipour

Physics Department and Biruni Observatory, College of Sciences, Shiraz University, Shiraz 71454, Iran
(Received 13 October 2015; published 12 January 2016)

In this paper, we analyze the dilepton mass square q^2 dependency of single lepton polarization asymmetries and CP violation for $\bar{B} \rightarrow \bar{K}_0^*(1430)\ell^+\ell^-$, $\ell = \mu, \tau$ in the two Higgs doublet model context. Also, we study the averages of these asymmetries in the domain $4m_\ell^2 < q^2 < (m_B - m_{K_0^*})^2$. Our study manifests that the investigation of the above-mentioned asymmetries for $\bar{B} \rightarrow \bar{K}_0^*(1430)\ell^+\ell^-$ processes could provide useful information for probing new Higgs bosons in the future B-physics experiments.

DOI: [10.1103/PhysRevD.93.015007](https://doi.org/10.1103/PhysRevD.93.015007)

I. INTRODUCTION

Now that the last missing ingredient of the Standard Model (SM) (SM Higgs particle) has been experimentally discovered at the LHC by the ATLAS [1] and CMS [2,3] collaborations, with a mass $m_H \approx 125$ GeV, the possibility of the discovery of an enlarged scalar sector becomes very plausible. On the other hand, between the spectrum of extensions of the SM, there are predictions that anticipate more than one scalar Higgs doublet; for instance, the case of the minimal supersymmetric Standard Model. Based on this, we can consider a prototype of extensions of the SM which include a larger scalar sector, called generically the two Higgs doublet model (2HDM). There are different types of such 2HDM models. In the model called type I, one Higgs doublet generates masses for the up and down quarks, simultaneously. In model type II, one Higgs doublet gives masses to the up-type quarks, and the other one gives masses to the down-type quarks. These two models include a discrete symmetry to prevent flavor-changing neutral currents (FCNC) at tree level. However, the addition of these discrete symmetries is not required, and in this case, both doublets are contributing to provide the masses to up-type and down-type quarks. In the literature, such a model is known as the 2HDM type III. It has been used to search for physics beyond the SM and specifically for FCNC at tree level. In general, both doublets can acquire a vacuum expectation value (VEV), but one of them can be absorbed redefining the Higgs boson fields properly. Nevertheless, other studies on 2HDM-III using a different basis have been done, and there is a case in which both doublets get VEVs that allow one to study model types I and II in a specific limit [4,5].

In the 2HDM models, the two complex Higgs doublets include eighth scalar states. A spontaneous symmetry breaking procedure generates five Higgs fields: two neutral CP -even scalars h^0 and H^0 , a neutral CP -odd scalar A^0 , and two charged scalars H . While the neutral Higgs bosons may be

difficult to distinguish from the one of the SM, the charged Higgs bosons would have a distinctive signal for physics beyond the SM. Therefore, the direct or indirect effect of a charged Higgs boson would play an important role in the discovery of an extended Higgs model. The limitations which come from the experimental results of $B-\bar{B}$ mixing, $\Gamma(b \rightarrow s\gamma)$, $\Gamma(b \rightarrow c\tau\bar{\nu}_\tau)$, ρ_0 , R_b and the electric dipole moments of the electron and neutron [5–8] could constrain the range of variation of masses of Higgs bosons and that of the other related parameters such as vertex parameters, λ_{tt} and λ_{bb} .

FCNC and CP violation are indeed the most sensitive probes of new physics (NP) contributions to penguin operators. Rare decays, induced by the FCNC of $b \rightarrow s\ell^+\ell^-$ ($\ell = e, \mu, \tau$) transitions are at the forefront of our quest to understand flavor and the origins of CP -violation asymmetry, offering one of the best probes for NP beyond the SM, in particular to explore 2HDM.

Although the branching ratios of FCNC decays are small in the SM, interesting results are yielded in developing experiments. The inclusive $b \rightarrow X_s\ell^+\ell^-$ decay is observed by the BABAR [9] and Belle collaborations. These collaborations also measured exclusive modes $B \rightarrow K\ell^+\ell^-$ [10–12] and $B \rightarrow K^*\ell^+\ell^-$ [13]. These experimental results show high agreement with theoretical predictions [14–16].

There exists another group of rare decays induced by $b \rightarrow s$ transition, such as $B \rightarrow K_2^*(1430)\ell^+\ell^-$ and $B \rightarrow K_0^*(1430)\ell^+\ell^-$ in which a B meson decays into a tensor or scalar meson, respectively. These decays are deeply investigated in the SM in Refs. [17,18], and the related transition form factors are formulated within the framework of light front quark model [18–20] and QCD sum rules method [21,22], respectively.

In this paper, we will investigate the exclusive decay $\bar{B} \rightarrow \bar{K}_0^*(1430)\ell^+\ell^-$ ($\ell = \mu, \tau$), where $\bar{K}_0^*(1430)$ is a scalar meson, both in the SM and 2HDM. We evaluate the single lepton polarization asymmetries and CP -violating effects with special emphasis on model III of the 2HDM.

The paper is organized as follows. In Sec. II, we describe the content of the general 2HDM and write down the

^{*}falahati@shirazu.ac.ir

Yukawa Lagrangian for model III. In Sec. III, the effective Hamiltonian and matrix elements of $\bar{B} \rightarrow \bar{K}_0^*(1430)\ell^+\ell^-$ transition in the SM and 2HDM are presented. Then, the general expressions for single lepton polarization asymmetries and CP violation have been extracted out. Section IV is devoted to discussion and our conclusions. In the final section, a brief summery of our results is presented.

II. GENERAL TWO HIGGS DOUBLET MODEL

In a general two Higgs doublet model, both the doublets can couple to the up-type and down-type quarks. Without missing anything, we use a basis such that the first doublet produces the masses of all the gauge bosons and fermions [5],

$$\langle \phi_1 \rangle = \begin{pmatrix} 0 \\ \frac{v}{\sqrt{2}} \end{pmatrix}, \quad \langle \phi_2 \rangle = 0, \quad (1)$$

where v is due to the W mass by $M_W = \frac{g}{2}v$. Based on this, the first doublet ϕ_1 is the same as the SM doublet, whereas all the new Higgs fields originate from the second doublet ϕ_2 . They are written as

$$\phi_1 = \frac{1}{\sqrt{2}} \begin{pmatrix} \sqrt{2}G^+ \\ v + \chi_1^0 + iG^0 \end{pmatrix}, \quad \phi_2 = \frac{1}{\sqrt{2}} \begin{pmatrix} \sqrt{2}H^+ \\ \chi_2^0 + iA^0 \end{pmatrix}, \quad (2)$$

where G^0 and G^\pm are the Goldstone bosons that would be absorbed in the Higgs mechanism to provide the longitudinal

components of the weak gauge bosons. The H^\pm are the physical charged-Higgs bosons, and A^0 is the physical CP -odd neutral Higgs boson. The χ_1^0 and χ_2^0 are not physical mass eigenstates but are written as linear combinations of the CP -even neutral Higgs bosons,

$$\chi_1^0 = H^0 \cos \alpha - h^0 \sin \alpha \quad (3)$$

$$\chi_2^0 = H^0 \sin \alpha + h^0 \cos \alpha, \quad (4)$$

where α is the mixing angle. Using this basis, the couplings of $\chi_2^0 ZZ$ and $\chi_2^0 W^+ W^-$ disappear. We can present [23] the Yukawa Lagrangian for model III as

$$-\mathcal{L}_Y = \eta_{ij}^U \overline{Q_{iL}} \tilde{\phi}_1 U_{jR} + \eta_{ij}^D \overline{Q_{iL}} \phi_1 D_{jR} + \xi_{ij}^U \overline{Q_{iL}} \tilde{\phi}_2 U_{jR} + \xi_{ij}^D \overline{Q_{iL}} \phi_2 D_{jR} + \text{H.c.}, \quad (5)$$

where i, j are generation indices; $\tilde{\phi}_{1,2} = i\sigma_2 \phi_{1,2}$; $\eta_{ij}^{U,D}$ and $\xi_{ij}^{U,D}$ are, in general, nondiagonal coupling matrices; Q_{iL} is the left-handed fermion doublet; and U_{jR} and D_{jR} are the right-handed singlets. Note that these Q_{iL} , U_{jR} and D_{jR} are weak eigenstates, which can be expanded by mass eigenstates. As we have mentioned above, ϕ_1 provides all the fermion masses, and, therefore, $\frac{v}{\sqrt{2}}\eta^{U,D}$ will become the up- and down-type quark-mass matrices after a biunitary transformation. Applying the transformation, the Yukawa Lagrangian becomes

$$\begin{aligned} \mathcal{L}_Y = & -\bar{U}M_U U - \bar{D}M_D D - \frac{g}{2M_W}(H^0 \cos \alpha - h^0 \sin \alpha)(\bar{U}M_U U + \bar{D}M_D D) + \frac{ig}{2M_W}G^0(\bar{U}M_U \gamma^5 U - \bar{D}M_D \gamma^5 D) \\ & + \frac{g}{\sqrt{2}M_W}G^- \bar{D}V_{\text{CKM}}^\dagger \left[M_U \frac{1}{2}(1 + \gamma^5) - M_D \frac{1}{2}(1 - \gamma^5) \right] U - \frac{g}{\sqrt{2}M_W}G^+ \bar{U}V_{\text{CKM}} \left[M_D \frac{1}{2}(1 + \gamma^5) - M_U \frac{1}{2}(1 - \gamma^5) \right] D \\ & - \frac{H^0 \sin \alpha + h^0 \cos \alpha}{\sqrt{2}} \left[\bar{U} \left(\hat{\xi}^U \frac{1}{2}(1 + \gamma^5) + \hat{\xi}^{U\dagger} \frac{1}{2}(1 - \gamma^5) \right) U + \bar{D} \left(\hat{\xi}^D \frac{1}{2}(1 + \gamma^5) + \hat{\xi}^{D\dagger} \frac{1}{2}(1 - \gamma^5) \right) D \right] \\ & + \frac{iA^0}{\sqrt{2}} \left[\bar{U} \left(\hat{\xi}^U \frac{1}{2}(1 + \gamma^5) - \hat{\xi}^{U\dagger} \frac{1}{2}(1 - \gamma^5) \right) U - \bar{D} \left(\hat{\xi}^D \frac{1}{2}(1 + \gamma^5) - \hat{\xi}^{D\dagger} \frac{1}{2}(1 - \gamma^5) \right) D \right] \\ & - H^+ \bar{U} \left[V_{\text{CKM}} \hat{\xi}^D \frac{1}{2}(1 + \gamma^5) - \hat{\xi}^{U\dagger} V_{\text{CKM}} \frac{1}{2}(1 - \gamma^5) \right] D - H^- \bar{D} \left[\hat{\xi}^{D\dagger} V_{\text{CKM}}^\dagger \frac{1}{2}(1 - \gamma^5) - V_{\text{CKM}}^\dagger \hat{\xi}^U \frac{1}{2}(1 + \gamma^5) \right] U, \quad (6) \end{aligned}$$

where U is a symbol for the mass eigenstates of u, c, t quarks and D is a symbol for the mass eigenstates of d, s, b quarks. The diagonal mass matrices are defined by $M_{U,D} = \text{diag}(m_{u,d}, m_{c,s}, m_{t,b}) = \frac{v}{\sqrt{2}}(\mathcal{L}_{U,D})^\dagger \eta^{U,D}(\mathcal{R}_{U,D})$, $\hat{\xi}^{U,D} = (\mathcal{L}_{U,D})^\dagger \xi^{U,D}(\mathcal{R}_{U,D})$. The Cabibbo-Kobayashi-Maskawa matrix [24] is given by $V_{\text{CKM}} = (\mathcal{L}_U)^\dagger(\mathcal{L}_D)$.

The matrices $\hat{\xi}^{U,D}$ contain the FCNC couplings. These matrices would be given as [25]

$$\hat{\xi}_{ij}^{U,D} = \lambda_{ij} \frac{g\sqrt{m_i m_j}}{\sqrt{2}M_W} \quad (7)$$

by which the quark-mass hierarchy is ensured while the FCNC for the first two generations is suppressed, is allowed for the third generation.

III. ANALYTIC FORMULAS

A. Effective Hamiltonian for $\bar{B} \rightarrow \bar{K}_0^*(1430)\ell^+\ell^-$ transition in SM and 2HDM

The exclusive decay $\bar{B} \rightarrow \bar{K}_0^*(1430)\ell^+\ell^-$ is described at the quark level by the $b \rightarrow s\ell^+\ell^-$ transition. Taking into account the additional Higgs boson exchange diagrams, the effective Hamiltonian is calculated in the 2HDM as

$$\mathcal{H}_{\text{eff}}(b \rightarrow s\ell^+\ell^-) = -\frac{4G_F}{\sqrt{2}}V_{tb}V_{ts}^* \left\{ \sum_{i=1}^{10} C_i(\mu)O_i(\mu) + \sum_{i=1}^{10} C_{Q_i}(\mu)Q_i(\mu) \right\}, \quad (8)$$

where the first set of operators in the brackets is due to the SM effective Hamiltonian. Also note that the contributions of charged Higgs diagrams are taken into account in the aforementioned set of operators by modifying the corresponding Wilson coefficients. The second part which includes new operators is extracted from the contribution of the massive neutral Higgs bosons to this decay. All operators as well as the related Wilson coefficients are given in Refs. [23,26,27]. Now, using the above effective Hamiltonian, the one-loop matrix elements of $b \rightarrow s\ell^+\ell^-$ can be given as

$$\begin{aligned} \mathcal{M} &= \langle s\ell^+\ell^- | \mathcal{H}_{\text{eff}} | b \rangle \\ &= -\frac{G_F\alpha}{2\sqrt{2}\pi}V_{tb}V_{ts}^* \left\{ \tilde{C}_9^{\text{eff}}\bar{s}\gamma_\mu(1-\gamma_5)b\bar{\ell}\gamma^\mu\ell + \tilde{C}_{10}\bar{s}\gamma_\mu(1-\gamma_5)b\bar{\ell}\gamma^\mu\gamma_5\ell - 2C_7^{\text{eff}}\frac{m_b}{q^2}\bar{s}i\sigma_{\mu\nu}q^\nu(1+\gamma_5)b\bar{\ell}\gamma^\mu\ell \right. \\ &\quad \left. - 2C_7^{\text{eff}}\frac{m_s}{q^2}\bar{s}i\sigma_{\mu\nu}q^\nu(1-\gamma_5)b\bar{\ell}\gamma^\mu\ell + C_{Q_1}\bar{s}(1+\gamma_5)b\bar{\ell}\ell + C_{Q_2}\bar{s}(1+\gamma_5)b\bar{\ell}\gamma_5\ell \right\}. \end{aligned} \quad (9)$$

The Wilson coefficients C_7^{eff} , \tilde{C}_9^{eff} , \tilde{C}_{10} are obtained from their SM values by adding the contributions due to the charged Higgs bosons exchange diagrams. Note that this addition is performed at the high m_W scale, and then using the renormalization group equations, the coefficients are calculated at the lower m_b scale. Coefficients C_{Q_1} and C_{Q_2} describe the neutral Higgs boson exchange diagrams' contributions. The operators O_i ($i = 1, \dots, 10$) do not mix with Q_1 and Q_2 , and there is no mixing between Q_1 and Q_2 . For this reason, the evolutions of the coefficients C_{Q_1} and C_{Q_2} are controlled by the anomalous dimensions of Q_1 and Q_2 , respectively [27],

$$C_{Q_i}(m_b) = \eta^{-\gamma_Q/\beta_0}C_{Q_i}(m_W), \quad i = 1, 2,$$

where $\gamma_Q = -4$ is the anomalous dimension of the operator $\bar{s}_L b_R$.

The coefficients $C_i(m_W)$ ($i = 7, 9$, and 10) and $C_{Q_1}(m_W)$ and $C_{Q_2}(m_W)$ are given by

$$\begin{aligned} C_7(m_W) &= x\frac{(7-5x-8x^2)}{24(x-1)^3} + \frac{x^2(3x-2)}{4(x-1)^4}\ln x + |\lambda_{tt}|^2 \left(\frac{y(7-5y-8y^2)}{72(y-1)^3} + \frac{y^2(3y-2)}{12(y-1)^4}\ln y \right) \\ &\quad + \lambda_{tt}\lambda_{bb} \left(\frac{y(3-5y)}{12(y-1)^2} + \frac{y(3y-2)}{6(y-1)^3}\ln y \right), \end{aligned} \quad (10)$$

$$\begin{aligned} C_9(m_W) &= -\frac{1}{\sin^2\theta_W}B(m_W) + \frac{1-4\sin^2\theta_W}{\sin^2\theta_W}C(m_W) + \frac{x^2(25-19x)}{36(x-1)^3} + \frac{-3x^4+30x^3-54x^2+32x-8}{18(x-1)^4}\ln x + \frac{4}{9} \\ &\quad + |\lambda_{tt}|^2 \left[\frac{1-4\sin^2\theta_W}{\sin^2\theta_W} \frac{xy}{8} \left(\frac{1}{y-1} - \frac{1}{(y-1)^2}\ln y \right) - y \left(\frac{47y^2-79y+38}{108(y-1)^3} - \frac{3y^3-6y^3+4}{18(y-1)^4}\ln y \right) \right], \end{aligned} \quad (11)$$

$$C_{10}(m_W) = \frac{1}{\sin^2\theta_W}(B(m_W) - C(m_W)) + |\lambda_{tt}|^2 \frac{1}{\sin^2\theta_W} \frac{xy}{8} \left(-\frac{1}{y-1} + \frac{1}{(y-1)^2}\ln y \right), \quad (12)$$

$$\begin{aligned} C_{Q_1}(m_W) &= \frac{m_b m_\ell}{m_{h^0}^2} \frac{1}{|\lambda_{tt}|^2} \frac{1}{\sin^2\theta_W} \frac{x}{4} \left\{ (\sin^2\alpha + h\cos^2\alpha)f_1(x, y) + \left[\frac{m_{h^0}^2}{m_W^2} + (\sin^2\alpha + h\cos^2\alpha)(1-z) \right] f_2(x, y) \right. \\ &\quad \left. + \frac{\sin^2 2\alpha}{2m_{H^\pm}^2} \left[m_{h^0}^2 - \frac{(m_{h^0}^2 + m_{H^0}^2)^2}{2m_{H^0}^2} \right] f_3(y) \right\}, \end{aligned} \quad (13)$$

$$C_{Q_2}(m_W) = -\frac{m_b m_\ell}{m_{A^0}^2} \frac{1}{|\lambda_{tt}|^2} \left\{ f_1(x, y) + \left[1 + \frac{m_{H^\pm}^2 - m_{A^0}^2}{m_W^2} \right] f_2(x, y) \right\}, \quad (14)$$

where

$$\begin{aligned}
x &= \frac{m_t^2}{m_W^2}, & y &= \frac{m_t^2}{m_{H^\pm}^2}, & z &= \frac{x}{y}, & h &= \frac{m_{h^0}^2}{m_{H^0}^2}, \\
B(x) &= -\frac{x}{4(x-1)} + \frac{x}{4(x-1)^2} \ln x, & C(x) &= \frac{x}{4} \left(\frac{x-6}{2(x-1)} + \frac{3x+2}{2(x-1)^2} \ln x \right), \\
f_1(x, y) &= \frac{x \ln x}{x-1} - \frac{y \ln y}{y-1}, \\
f_2(x, y) &= \frac{x \ln y}{(z-x)(x-1)} + \frac{\ln z}{(z-1)(x-1)}, \\
f_3(y) &= \frac{1-y+y \ln y}{(y-1)^2}.
\end{aligned} \tag{15}$$

It should be noted that the coefficient $\tilde{C}_9^{\text{eff}}(\mu)$ can be written by three parts,

$$\tilde{C}_9^{\text{eff}}(\mu) = \tilde{C}_9(\mu) + Y_{\text{SD}}(\hat{m}_c, \hat{s}) + Y_{\text{LD}}(\hat{m}_c, \hat{s}), \tag{16}$$

where the parameters \hat{m}_c and \hat{s} are defined as $\hat{m}_c = m_c/m_b$, $\hat{s} = q^2/m_b^2$. $Y_{\text{SD}}(\hat{m}_c, \hat{s})$ describes the short-distance contributions from four-quark operators which can be calculated in the perturbative theory. The function $Y_{\text{SD}}(\hat{m}_c, \hat{s})$ is given by

$$\begin{aligned}
Y_{\text{SD}} &= g(\hat{m}_c, \hat{s})(3C_1 + C_2 + 3C_3 + C_4 + 3C_5 + C_6) - \frac{1}{2}g(1, \hat{s})(4C_3 + 4C_4 + 3C_5 + C_6) \\
&\quad - \frac{1}{2}g(0, \hat{s})(C_3 + 3C_4) + \frac{2}{9}(3C_3 + C_4 + 3C_5 + C_6),
\end{aligned} \tag{17}$$

where the explicit expressions for the g functions can be found in Ref. [26]. The long-distance contributions $Y_{\text{LD}}(\hat{m}_c, \hat{s})$ originate from the real $c\bar{c}$ intermediate states, i.e., $J/\psi, \psi', \dots$. The J/ψ family is introduced by the Breit-Wigner distribution for the resonances through the function [28,29]

$$Y_{\text{LD}} = \frac{3\pi}{\alpha^2} C^{(0)} \sum_{V_i=J/\psi, \psi', \dots} k_i \frac{\Gamma(V_i \rightarrow \ell^+ \ell^-) m_{V_i}}{m_{V_i}^2 - q^2 - im_{V_i} \Gamma_{V_i}},$$

where α is the fine structure constant and $C^{(0)} = (3C_1 + C_2 + 3C_3 + C_4 + 3C_5 + C_6)$. The phenomenological parameters k_i for the $\bar{B} \rightarrow \bar{K}_0^*(1430)\ell^+\ell^-$ decay can be fixed from $\text{Br}(\bar{B} \rightarrow J/\psi \bar{K}_0^*(1430) \rightarrow \bar{K}_0^*(1430)\ell^+\ell^-) = \text{Br}(\bar{B} \rightarrow J/\psi \bar{K}_0^*(1430)) \times \text{Br}(J/\psi \rightarrow \ell^+\ell^-)$. However, since the branching ratio of the $\bar{B} \rightarrow J/\psi \bar{K}_0^*(1430)$ decay has not been measured yet, we assume that the values of k_i are in the order of 1. Therefore, we use $k_1 = k_2 = 1$ in the following numerical calculations [29].

B. Form factors for $\bar{B} \rightarrow \bar{K}_0^*(1430)\ell^+\ell^-$ transition

The exclusive $\bar{B} \rightarrow \bar{K}_0^*(1430)\ell^+\ell^-$ decay is described in terms of the matrix elements of the quark operators in Eq. (9) over meson states, which can be parametrized in terms of the form factors. The needed matrix elements for the calculation of the $\bar{B} \rightarrow \bar{K}_0^*(1430)\ell^+\ell^-$ decay are

$$\langle \bar{K}_0^*(1430)(p_{K_0^*}) | \bar{s} \gamma_\mu (1 \pm \gamma_5) b | \bar{B}(p_B) \rangle = \pm [f_+(q^2)(p_B + p_{K_0^*})_\mu + f_-(q^2)q_\mu], \tag{18}$$

$$\langle \bar{K}_0^*(1430)(p_{K_0^*}) | \bar{s} i \sigma_{\mu\nu} q^\nu (1 \pm \gamma_5) b | \bar{B}(p_B) \rangle = \frac{\pm f_T(q^2)}{m_B + m_{K_0^*}} [(p_B + p_{K_0^*})_\mu q^2 - (m_B^2 - m_{K_0^*}^2)q_\mu], \tag{19}$$

$$\begin{aligned}
\langle \bar{K}_0^*(1430)(p_{K_0^*}) | \bar{s} (1 \pm \gamma_5) b | \bar{B}(p_B) \rangle &= \pm \langle \bar{K}_0^*(1430)(p_{K_0^*}) | \bar{s} \gamma_5 b | \bar{B}(p_B) \rangle = \mp \frac{1}{m_b + m_s} [f_+(q^2)(p_B + p_{K_0^*}) \cdot q + f_-(q^2)q^2] \\
&= \mp \frac{f_0(q^2)}{m_b + m_s} (m_B^2 - m_{K_0^*}^2),
\end{aligned} \tag{20}$$

$$\langle \bar{K}_0^*(1430)(p_{K_0^*}) | \bar{s} b | \bar{B}(p_B) \rangle = 0, \tag{21}$$

where $q = p_B - p_{K_0^*}$ and the function $f_0(q^2)$ has been extracted from

TABLE I. Form factors for $\bar{B} \rightarrow \bar{K}_0^*(1430)$ transition obtained within three-point QCD sum rules are fitted to the three-parameter form.

F	$F(0)$	a_F	b_F
$f_+^{\bar{B} \rightarrow \bar{K}_0^*}$	0.31 ± 0.08	0.81	-0.21
$f_-^{\bar{B} \rightarrow \bar{K}_0^*}$	-0.31 ± 0.07	0.80	-0.36
$f_T^{\bar{B} \rightarrow \bar{K}_0^*}$	-0.26 ± 0.07	0.41	-0.32

$$f_-(q^2) = \frac{(m_B^2 - m_{K_0^*}^2)}{q^2} [f_0(q^2) - f_+(q^2)]. \quad (22)$$

For the form factors, we have used the results of three-point QCD sum rules method [21] in which the q^2 dependence of all form factors is given by

$$F(q^2) = \frac{F(0)}{1 - a_F(q^2/m_B^2) + b_F(q^2/m_B^2)^2}, \quad (23)$$

where the values of parameters $F(0)$, a_F , and b_F for the $\bar{B} \rightarrow \bar{K}_0^*(1430)\ell^+\ell^-$ decay are exhibited in Table I.

C. Lepton polarization asymmetries and the CP -violating asymmetry of $\bar{B} \rightarrow \bar{K}_0^*(1430)\ell^+\ell^-$

Making use of Eq. (9) and the definitions of form factors, the matrix element of the $\bar{B} \rightarrow \bar{K}_0^*(1430)\ell^+\ell^-$ decay can be written as

$$\begin{aligned} \mathcal{M} = & \frac{G_F \alpha_{\text{em}}}{4\sqrt{2}\pi} V_{ts}^* V_{tb} m_B \{ [\mathcal{A}(p_B + p_{K_0^*}) + \mathcal{B}q]_\mu \bar{\ell} \gamma^\mu \ell \\ & + [\mathcal{C}(p_B + p_{K_0^*}) + \mathcal{D}q]_\mu \bar{\ell} \gamma^\mu \gamma_5 \ell \\ & + [\mathcal{Q}] \bar{\ell} \ell + [\mathcal{N}] \bar{\ell} \gamma_5 \ell \}, \end{aligned} \quad (24)$$

where the auxiliary functions $\mathcal{A}, \dots, \mathcal{Q}$ are listed in the following:

$$\mathcal{A} = -2\tilde{C}_9^{\text{eff}} f_+(q^2) - 4(m_b + m_s) C_7^{\text{eff}} \frac{f_T(q^2)}{m_B + m_{K_0^*}}, \quad (25)$$

$$\begin{aligned} \mathcal{B} = & -2\tilde{C}_9^{\text{eff}} f_-(q^2) \\ & + 4(m_b + m_s) C_7^{\text{eff}} \frac{f_T(q^2)}{(m_B + m_{K_0^*}) q^2} (m_B^2 - m_{K_0^*}^2), \end{aligned} \quad (26)$$

$$\mathcal{C} = -2\tilde{C}_{10} f_+(q^2), \quad (27)$$

$$\mathcal{D} = -2\tilde{C}_{10} f_-(q^2), \quad (28)$$

$$\mathcal{Q} = -2C_{Q_1} f_0(q^2) \frac{(m_B^2 - m_{K_0^*}^2)}{m_b + m_s}, \quad (29)$$

$$\mathcal{N} = -2C_{Q_2} f_0(q^2) \frac{(m_B^2 - m_{K_0^*}^2)}{m_b + m_s}, \quad (30)$$

with $q = p_B - p_{K_0^*} = p_{\ell^+} + p_{\ell^-}$.

The unpolarized differential decay rate for the $\bar{B} \rightarrow \bar{K}_0^*(1430)\ell^+\ell^-$ decay in the rest frame of the B meson is given by

$$\frac{d\Gamma(\bar{B} \rightarrow K_0^* \ell^+ \ell^-)}{d\hat{s}} = -\frac{G_F^2 \alpha_{\text{em}}^2 m_B}{2^{14} \pi^5} |V_{tb} V_{ts}^*|^2 v \sqrt{\lambda} \Delta, \quad (31)$$

with

$$\begin{aligned} \Delta = & 16m_\ell m_B^2 (1 - \hat{r}_{K_0^*}) \text{Re}[\mathcal{C}\mathcal{N}^*] + 4\hat{s} m_B^2 v^2 |\mathcal{Q}|^2 \\ & + 16\hat{s} m_\ell^2 m_B^2 |\mathcal{D}|^2 + 32m_\ell^2 m_B^2 (1 - \hat{r}_{K_0^*}) \text{Re}[\mathcal{C}\mathcal{D}^*] \\ & + 16\hat{s} m_\ell m_B^2 \text{Re}[\mathcal{D}\mathcal{N}^*] + 2\hat{s} m_B^2 |\mathcal{N}|^2 \\ & + \frac{4}{3} m_B^4 \lambda (3 - v^2) |\mathcal{A}|^2 \\ & + \frac{4}{3} m_B^4 |\mathcal{C}|^2 \{2\lambda - (1 - v^2)(2\lambda - 3(1 - \hat{r}_{K_0^*})^2)\}, \end{aligned} \quad (32)$$

where $v = \sqrt{1 - 4m_\ell^2/q^2}$, $\hat{s} = q^2/m_B^2$, $\hat{r}_{K_0^*} = m_{K_0^*}^2/m_B^2$, and $\lambda = 1 + \hat{r}_{K_0^*}^2 + \hat{s}^2 - 2\hat{s} - 2\hat{r}_{K_0^*}(1 + \hat{s})$.

The CP -violating asymmetry of the $\bar{B} \rightarrow \bar{K}_0^*(1430)\ell^+\ell^-$ decay is defined by

$$\mathcal{A}_{CP}(\hat{s}) = \frac{\frac{d\Gamma}{d\hat{s}} - \frac{d\bar{\Gamma}}{d\hat{s}}}{\frac{d\Gamma}{d\hat{s}} + \frac{d\bar{\Gamma}}{d\hat{s}}}, \quad (33)$$

where $\frac{d\Gamma}{d\hat{s}}$ is the unpolarized differential decay rate given by Eq. (31) and $\frac{d\bar{\Gamma}}{d\hat{s}}$ is the unpolarized differential decay rate for the antiparticle channel. To obtain the latter one, we should change the parameters $V_{ts}^* V_{tb}$, λ_{it} , and λ_{it}^* of the former one into $V_{ts} V_{tb}^*$, λ_{it}^* , and λ_{it} .

Having obtained the CP -violation asymmetry, let us now consider the single lepton polarization asymmetries associated with the polarized leptons. For this purpose, we first define the following orthogonal unit vectors $s_i^{\pm\mu}$ in the rest frame of ℓ^\pm , where $i = L, N$, or T are the abbreviations of the longitudinal, normal, and transversal spin projections, respectively,

$$\begin{aligned}
 s_L^{-\mu} &= (0, \vec{e}_L^-) = \left(0, \frac{\vec{p}_{\ell^-}}{|\vec{p}_{\ell^-}|}\right), \\
 s_N^{-\mu} &= (0, \vec{e}_N^-) = \left(0, \frac{\vec{p}_{K_0^*} \times \vec{p}_{\ell^-}}{|\vec{p}_{K_0^*} \times \vec{p}_{\ell^-}|}\right), \\
 s_T^{-\mu} &= (0, \vec{e}_T^-) = (0, \vec{e}_N^- \times \vec{e}_L^-), \\
 s_L^{+\mu} &= (0, \vec{e}_L^+) = \left(0, \frac{\vec{p}_{\ell^+}}{|\vec{p}_{\ell^+}|}\right), \\
 s_N^{+\mu} &= (0, \vec{e}_N^+) = \left(0, \frac{\vec{p}_{K_0^*} \times \vec{p}_{\ell^+}}{|\vec{p}_{K_0^*} \times \vec{p}_{\ell^+}|}\right), \\
 s_T^{+\mu} &= (0, \vec{e}_T^+) = (0, \vec{e}_N^+ \times \vec{e}_L^+),
 \end{aligned} \tag{34}$$

where \vec{p}_{ℓ^\mp} and $\vec{p}_{K_0^*}$ are in the c.m. frame of the $\ell^-\ell^+$ system. Lorentz transformation is used to boost the

components of the lepton polarization to the c.m. frame of the lepton pair as

$$\begin{aligned}
 (s_L^{\mp\mu})_{CM} &= \left(\frac{|\vec{p}_{\ell^\mp}|}{m_\ell}, \frac{E_\ell \vec{p}_{\ell^\mp}}{m_\ell |\vec{p}_{\ell^\mp}|}\right), \\
 (s_N^{\mp\mu})_{CM} &= (s_N^{\mp\mu})_{RF}, \\
 (s_T^{\mp\mu})_{CM} &= (s_T^{\mp\mu})_{RF},
 \end{aligned} \tag{35}$$

where RF refers to the rest frame of the corresponding lepton as well as $\vec{p}_{\ell^+} = -\vec{p}_{\ell^-}$ and E_ℓ and m_ℓ are the energy and mass of leptons in the c.m. frame, respectively.

The single lepton polarization asymmetries can be defined as

$$\mathcal{P}_i^-(\hat{s}) = \frac{\left(\frac{d\Gamma}{d\hat{s}}(s_i^-, s_i^+) + \frac{d\Gamma}{d\hat{s}}(s_i^-, -s_i^+)\right) - \left(\frac{d\Gamma}{d\hat{s}}(-s_i^-, s_i^+) + \frac{d\Gamma}{d\hat{s}}(-s_i^-, -s_i^+)\right)}{\left(\frac{d\Gamma}{d\hat{s}}(s_i^-, s_i^+) + \frac{d\Gamma}{d\hat{s}}(s_i^-, -s_i^+)\right) + \left(\frac{d\Gamma}{d\hat{s}}(-s_i^-, s_i^+) + \frac{d\Gamma}{d\hat{s}}(-s_i^-, -s_i^+)\right)}, \tag{36}$$

$$\mathcal{P}_i^+(\hat{s}) = \frac{\left(\frac{d\Gamma}{d\hat{s}}(s_i^-, s_i^+) + \frac{d\Gamma}{d\hat{s}}(-s_i^-, s_i^+)\right) - \left(\frac{d\Gamma}{d\hat{s}}(s_i^-, -s_i^+) + \frac{d\Gamma}{d\hat{s}}(-s_i^-, -s_i^+)\right)}{\left(\frac{d\Gamma}{d\hat{s}}(s_i^-, s_i^+) + \frac{d\Gamma}{d\hat{s}}(s_i^-, -s_i^+)\right) + \left(\frac{d\Gamma}{d\hat{s}}(-s_i^-, s_i^+) + \frac{d\Gamma}{d\hat{s}}(-s_i^-, -s_i^+)\right)}, \tag{37}$$

where $\frac{d\Gamma(\hat{s})}{d\hat{s}}$'s are calculated in the c.m. frame. Using these definitions for the single lepton polarization asymmetries, the following explicit forms for \mathcal{P}_i^\pm 's are obtained:

$$\mathcal{P}_L^\mp = \frac{4vm_B^2}{\Delta} \left\{ \pm \frac{4}{3} \lambda m_B^2 \text{Re}[\mathcal{A}\mathcal{C}^*] - 4m_\ell(1 - \hat{r}_{K_0^*})\text{Re}[\mathcal{C}\mathcal{Q}^*] - 4m_\ell \hat{s} \text{Re}[\mathcal{D}\mathcal{Q}^*] - 2\hat{s} \text{Re}[\mathcal{N}\mathcal{Q}^*] \right\}, \tag{38}$$

$$\mathcal{P}_N^\mp = \frac{2\pi v \sqrt{\lambda \hat{s}} m_B^3}{\Delta} \left\{ +2m_\ell \text{Im}[\mathcal{D}\mathcal{C}^*] + \text{Im}[\mathcal{N}\mathcal{C}^*] \mp \text{Im}[\mathcal{A}\mathcal{Q}^*] \right\}, \tag{39}$$

$$\mathcal{P}_T^\mp = \frac{\pi \sqrt{\lambda \hat{s}} m_B^3}{\Delta} \left\{ \pm 2\text{Re}[\mathcal{A}\mathcal{N}^*] \pm \frac{4m_\ell}{\hat{s}}(1 - \hat{r}_{K_0^*})\text{Re}[\mathcal{A}\mathcal{C}^*] \pm 4m_\ell \text{Re}[\mathcal{A}\mathcal{D}^*] + 2v^2 \text{Re}[\mathcal{C}\mathcal{Q}^*] \right\}. \tag{40}$$

IV. NUMERICAL ANALYSIS

In this section, we would like to study the asymmetries \mathcal{A}_{CP} and \mathcal{P}_i^\pm 's and their averages for the exclusive decay $\bar{B} \rightarrow \bar{K}_0^*(1430)\ell^+\ell^-$ in the SM and model III of the 2HDM. The constraints on 2HDM parameters come from the experimental limits of the electric dipole moments of the neutron, $B^0 - \bar{B}^0$ mixing, ρ_0 , R_b , and $\text{Br}(b \rightarrow s\gamma)$ [5–8]. A simple ansatz for $\lambda_{tt}\lambda_{bb}$ would be

$$\lambda_{tt}\lambda_{bb} = |\lambda_{tt}\lambda_{bb}|e^{i\theta}. \tag{41}$$

Considering the restrictions of the above references on the parameters of model III of the 2HDM and taking $\theta = \pi/2$,

we use the following three classes of parameters throughout the numerical analysis [5]:

$$\begin{aligned}
 \text{CaseA: } & |\lambda_{tt}| = 0.03; & |\lambda_{bb}| &= 100, \\
 \text{CaseB: } & |\lambda_{tt}| = 0.15; & |\lambda_{bb}| &= 50, \\
 \text{CaseC: } & |\lambda_{tt}| = 0.3; & |\lambda_{bb}| &= 30.
 \end{aligned} \tag{42}$$

In addition, in this study, we have applied four sets of masses of Higgs bosons which are displayed in Table II [5].

The corresponding averages are defined by the equation [30]

TABLE II. List of the values for the masses of the Higgs particles.

	m_{H^\pm} GeV	m_{A^0} GeV	m_{h^0} GeV	m_{H^0} GeV
Mass set-1	200	125	125	160
Mass set-2	160	125	125	160
Mass set-3	200	125	125	125
Mass set-4	160	125	125	125

$$\langle \mathcal{A} \rangle = \frac{\int_{4\hat{m}_\ell^2}^{(1-\sqrt{\hat{r}_M})^2} \mathcal{A} \frac{dB}{d\hat{s}} d\hat{s}}{\int_{4\hat{m}_\ell^2}^{(1-\sqrt{\hat{r}_M})^2} \frac{dB}{d\hat{s}} d\hat{s}}, \quad (43)$$

where the subscript M refers to the $\bar{K}_0^*(1430)$ meson and the subscript \mathcal{A} refers to the asymmetries \mathcal{A}_{CP} and \mathcal{P}_i^\pm 's. The full kinematical interval of the dilepton invariant mass q^2 is $4m_\ell^2 \leq q^2 \leq (m_B - m_M)^2$, for which the long-distance

contributions (the charmonium resonances) can give substantial effects by considering the two low-lying resonances J/ψ and ψ' , in the interval of $8 \text{ GeV}^2 \leq q^2 \leq 14 \text{ GeV}^2$. To decrease the hadronic uncertainties, we use the kinematical region of q^2 for the muon as [29]

- I $4m_\ell^2 \leq q^2 \leq (m_{J/\psi} - 0.02 \text{ GeV})^2$,
- II $(m_{J/\psi} + 0.02 \text{ GeV})^2 \leq q^2 \leq (m_{\psi'} - 0.02 \text{ GeV})^2$,
- III $(m_{\psi'} + 0.02 \text{ GeV})^2 \leq q^2 \leq (m_B - m_M)^2$

and for tau as

- I $4m_\ell^2 \leq q^2 \leq (m_{\psi'} - 0.02 \text{ GeV})^2$,
- II $(m_{\psi'} + 0.02 \text{ GeV})^2 \leq q^2 \leq (m_B - m_M)^2$.

We continue our analysis regarding the \mathcal{A} 's and their averages by plotting a set of Figs. 1–11 and the

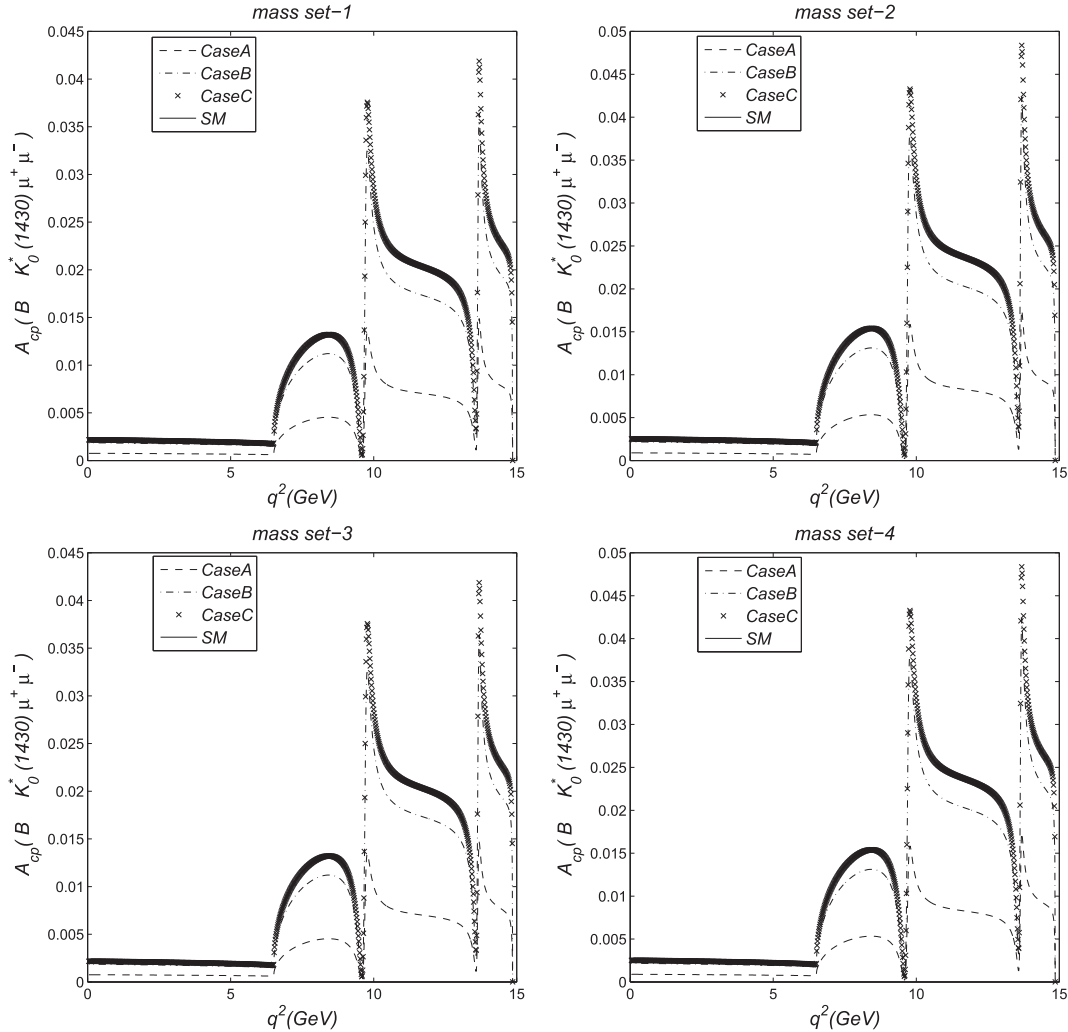


FIG. 1. The dependence of the \mathcal{A}_{CP} polarization on q^2 and the three typical cases of the 2HDM, i.e., cases A, B, and C, and the SM for the μ channel of $\bar{B} \rightarrow \bar{K}_0^*$ transition for mass sets 1, 2, 3, and 4.

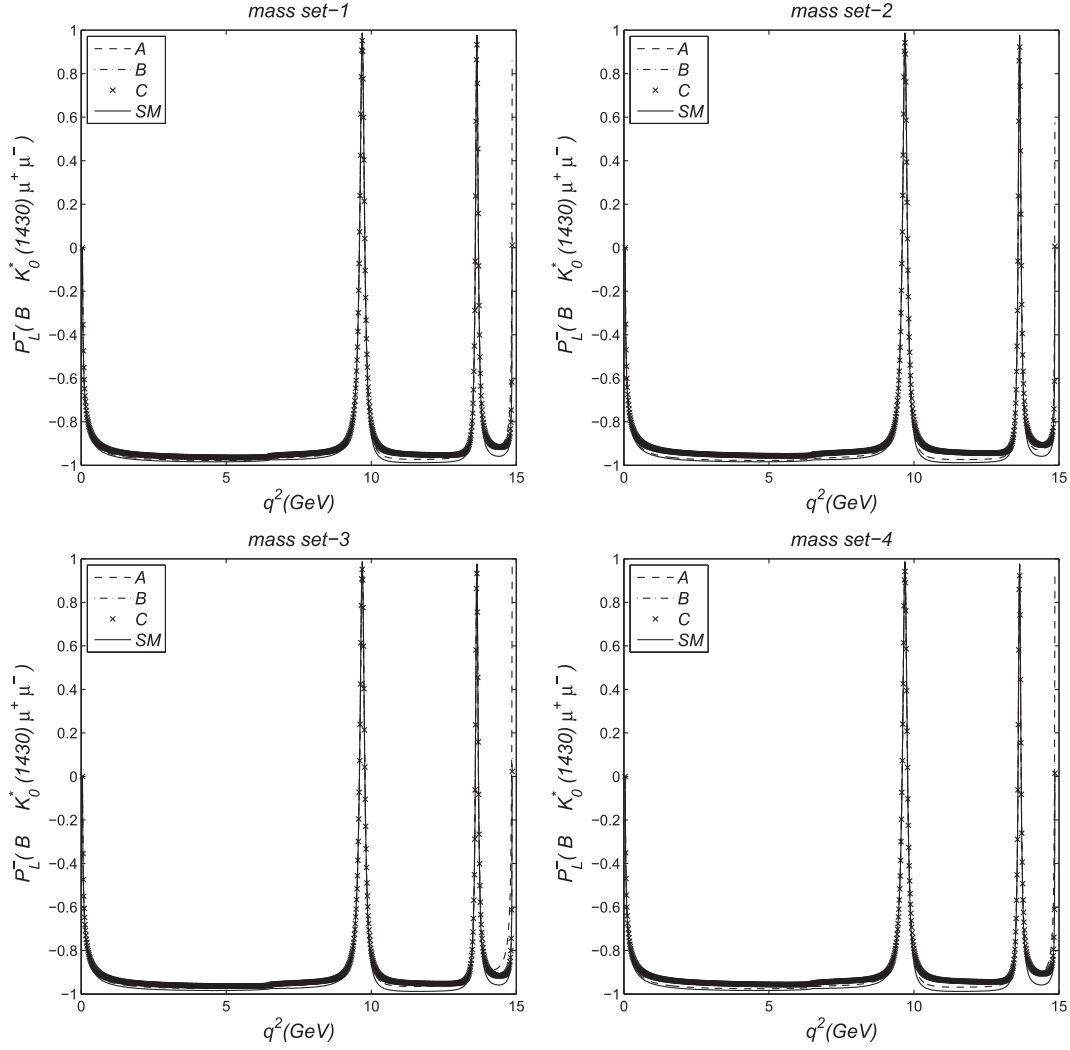


FIG. 2. The dependence of the \mathcal{P}_L^- polarization on q^2 and the three typical cases of the 2HDM, i.e., cases A, B, and C, and the SM for the μ channel of $\bar{B} \rightarrow \bar{K}_0^* \mu^+ \mu^-$ transition for mass sets 1, 2, 3, and 4.

presentation of a class of Tables III–VI. In these tables, the theoretical and experimental uncertainties corresponding to the SM averages have been evaluated. In such a manner, the theoretical uncertainties are extracted from the hadronic uncertainties related to the form factors, and the experimental uncertainties originate from the mass of quarks and hadrons and Wolfenstein parameters.

- (i) Analysis of \mathcal{A}_{CP} asymmetry for $\bar{B} \rightarrow \bar{K}_0^* \mu^+ \mu^-$ decay: The relevant plots in Fig. 1 show that, while the SM prediction of this asymmetry is zero, it is quite sensitive to the variation of the parameters λ_{tt} and λ_{bb} . For example, by enhancing the magnitude of $|\lambda_{tt}\lambda_{bb}|$, the deviation from the SM value is increased. Also, this asymmetry is quite sensitive to the variation of mass of H^\pm ; this happens due to the reduction of mass of H^\pm , such that the deviations from the SM value in mass sets

2 and 4 are more than those in mass sets 1 and 3. By combining the above analyses, it is understood that the most deviations from the SM prediction occur in the case C of mass sets 2 and 4. Next to $q^2 = m_{\psi'}^2$ in the aforementioned case and mass sets, a deviation around +0.05 is possible as compared to the zero expectation of the SM. In addition, it is found out through the corresponding Tables III and IV that the values of averages show ignorable sensitivities to the presence of new Higgs bosons.

- (ii) Analysis of \mathcal{P}_L^\mp asymmetries for $\bar{B} \rightarrow \bar{K}_0^* \mu^+ \mu^-$ decay: As it is obvious from Fig. 2, the predictions of all of mass sets throughout the domain $4m_\mu^2 \leq q^2 < (m_B - m_{K_0^*})^2$ apart from $q^2 = (m_B - m_{K_0^*})^2$ are the same and highly coincide with the SM prediction. At $q^2 = (m_B - m_{K_0^*})^2$, the deviation

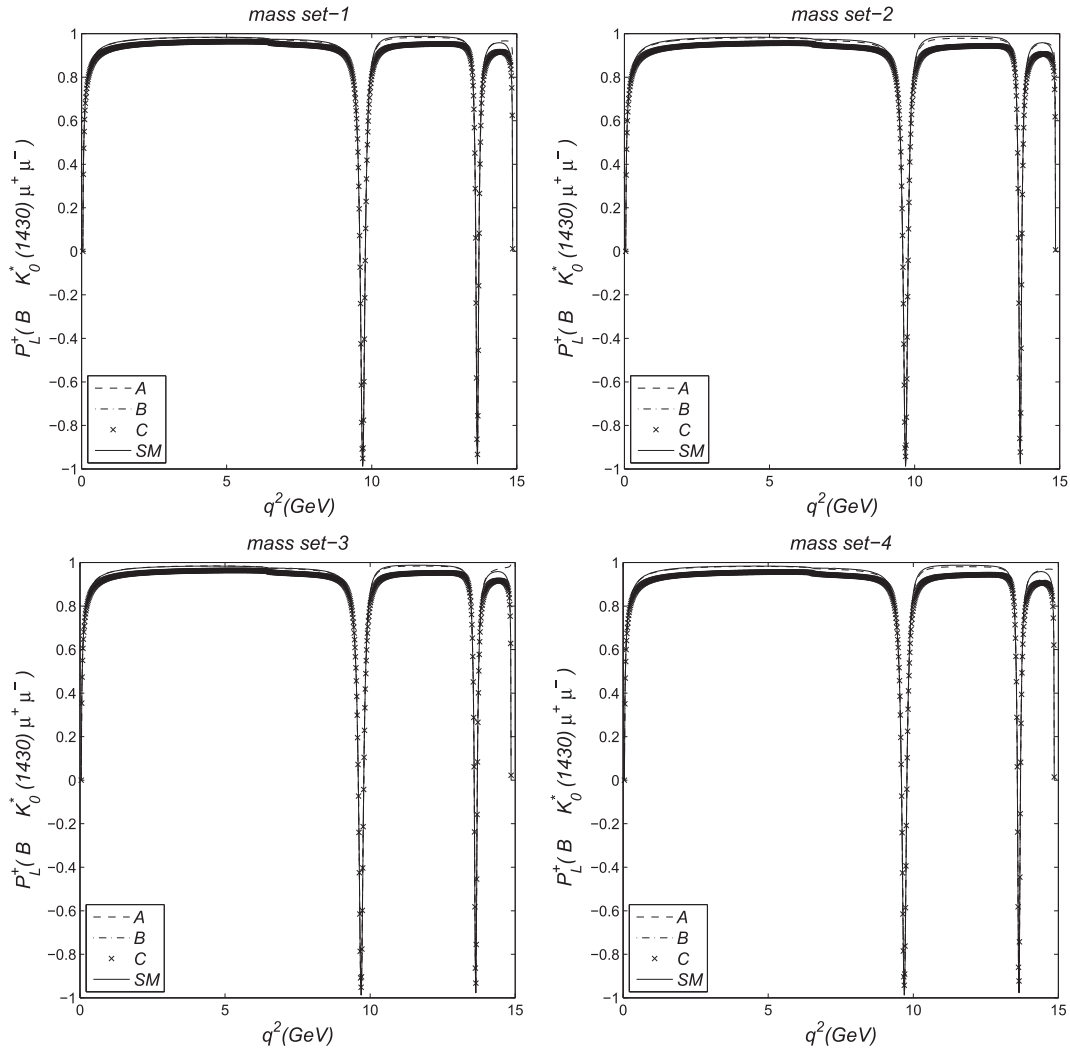


FIG. 3. The dependence of the \mathcal{P}_L^+ polarization on q^2 and the three typical cases of the 2HDM, i.e., cases A, B, and C, and the SM for the μ channel of $\bar{B} \rightarrow \bar{K}_0^* \mu^+ \mu^-$ transition for mass sets 1, 2, 3, and 4.

from the SM value in case A of mass set 3 is more than the others, which is $+1$. At such a point, the SM prediction is zero. Moreover, it is seen from Tables III and IV that the most deviations of $\langle \mathcal{P}_L^- \rangle$ from the calculated SM value happen in case C of mass sets 2 and 4 and are very small compared to the SM prediction (-3.2% SM). Also, it is clear from Eq. (38) that, while by ignoring the signs of \mathcal{P}_L^- and \mathcal{P}_L^+ in SM the magnitudes of them are the same ($\mathcal{P}_L^+ = -\mathcal{P}_L^-$ in the SM), those asymmetries do not have any symmetrical relationship with each other in the 2HDM. As it is obvious from Fig. 3 as well as Tables III and IV the predictions of all of mass sets and cases throughout the interval $4m_\mu^2 \leq q^2 \leq (m_B - m_{K_0^*})^2$ coincide with that of the SM very much. The most deviations of $\langle \mathcal{P}_L^+ \rangle$ from the calculated SM value happen in case C of mass sets

2 and 4 and are -3.2% SM. Ignoring $q^2 = (m_B - m_{K_0^*})^2$ and using the mentioned parameter space for the 2HDM, it is found out that $\mathcal{P}_L^+ = -\mathcal{P}_L^-$ in both the SM and 2HDM.

- (iii) Analysis of \mathcal{P}_N^\mp asymmetries for $\bar{B} \rightarrow \bar{K}_0^* \mu^+ \mu^-$ decay: The relevant plots in Fig. 4 show that this asymmetry is quite sensitive to the variation of the parameters λ_{tt} and λ_{bb} . For example, by decreasing the magnitude of $|\lambda_{tt}\lambda_{bb}|$, the deviation from the SM value is increased. Also, this asymmetry is quite sensitive to the variation of the masses of H^0 and H^\pm ; this happens due to the reduction of the mass of H^0 and the increment of the mass of H^\pm , such that the deviations from the SM value in mass sets 3 and 4 are more than those in mass sets 1 and 2. By combining the above analyses, it is understood that the most deviation from the SM

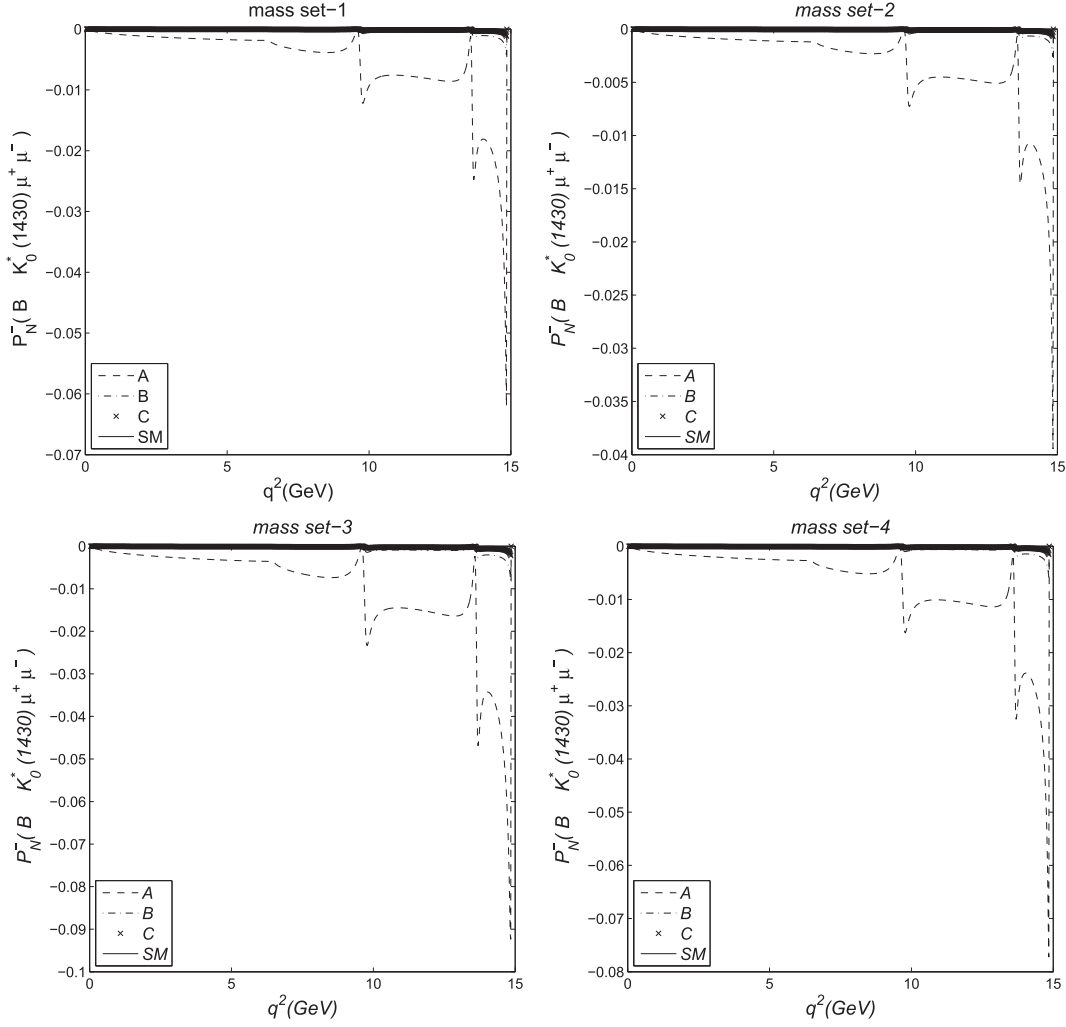


FIG. 4. The dependence of the \mathcal{P}_N^- polarization on q^2 and the three typical cases of the 2HDM, i.e., cases A, B, and C, and the SM for the μ channel of $\bar{B} \rightarrow \bar{K}_0^* \mu^+ \mu^-$ transition for mass sets 1, 2, 3, and 4.

prediction occurs in case A of mass set 3. Next to $q^2 = (m_B - m_{K_0^*})^2$ in the aforementioned case and mass set, a deviation around -0.09 is possible as compared to the SM expectation of zero asymmetry. In addition, it is found out through the corresponding tables that the values of averages show ignorable dependencies to the existence of new Higgs bosons. Moreover, it is clear from Eq. (39) that in the SM $\mathcal{P}_N^+ = \mathcal{P}_N^- = 0$, and in the 2HDM $\mathcal{P}_N^+ = -\mathcal{P}_N^-$.

- (iv) Analysis of \mathcal{P}_T^\mp asymmetries for $\bar{B} \rightarrow \bar{K}_0^* \mu^+ \mu^-$ decay: It is found out from Figs. 4–6 that the asymmetries \mathcal{P}_T^\mp and \mathcal{P}_N^\mp show similar sensitivities to the variations of mass sets and cases. For example, in these asymmetries, by decreasing the magnitude of $|\lambda_{tt}\lambda_{bb}|$ or the mass of H^0 and increasing the mass of H^\pm , the deviations from the SM predictions increase. According to this, the largest deviations from the SM predictions arise in case A of mass set

3. Next to $q^2 = (m_B - m_{K_0^*})^2$ in the mentioned case and mass set, deviations around +50% SM and -100% SM are possible for \mathcal{P}_T^- and \mathcal{P}_T^+ , respectively. In addition, it is found out through the corresponding tables that the most deviations of $\langle \mathcal{P}_T^- \rangle$ and $\langle \mathcal{P}_T^+ \rangle$ from the calculated SM values which happen in case A of mass set 3 are +24% SM and -22% SM, respectively. Moreover, it is clear from Eq. (40) while in SM there exists a symmetrical relationship between \mathcal{P}_T^- and \mathcal{P}_T^+ ($\mathcal{P}_T^- = -\mathcal{P}_T^+$), there not exist any symmetrical relationship between them in 2HDM. Nevertheless, it is evident from the relevant figures and tables that in cases B and C to a large extent $\mathcal{P}_T^+ = -\mathcal{P}_T^-$.

- (v) Analysis of \mathcal{A}_{CP} asymmetry for $\bar{B} \rightarrow \bar{K}_0^* \tau^+ \tau^-$ decay: The relevant plots in Fig. 7 show that, while the SM prediction of this asymmetry is zero, it is quite sensitive to the variation of the parameters λ_{tt} and λ_{bb} . For example, by enhancing the magnitude of

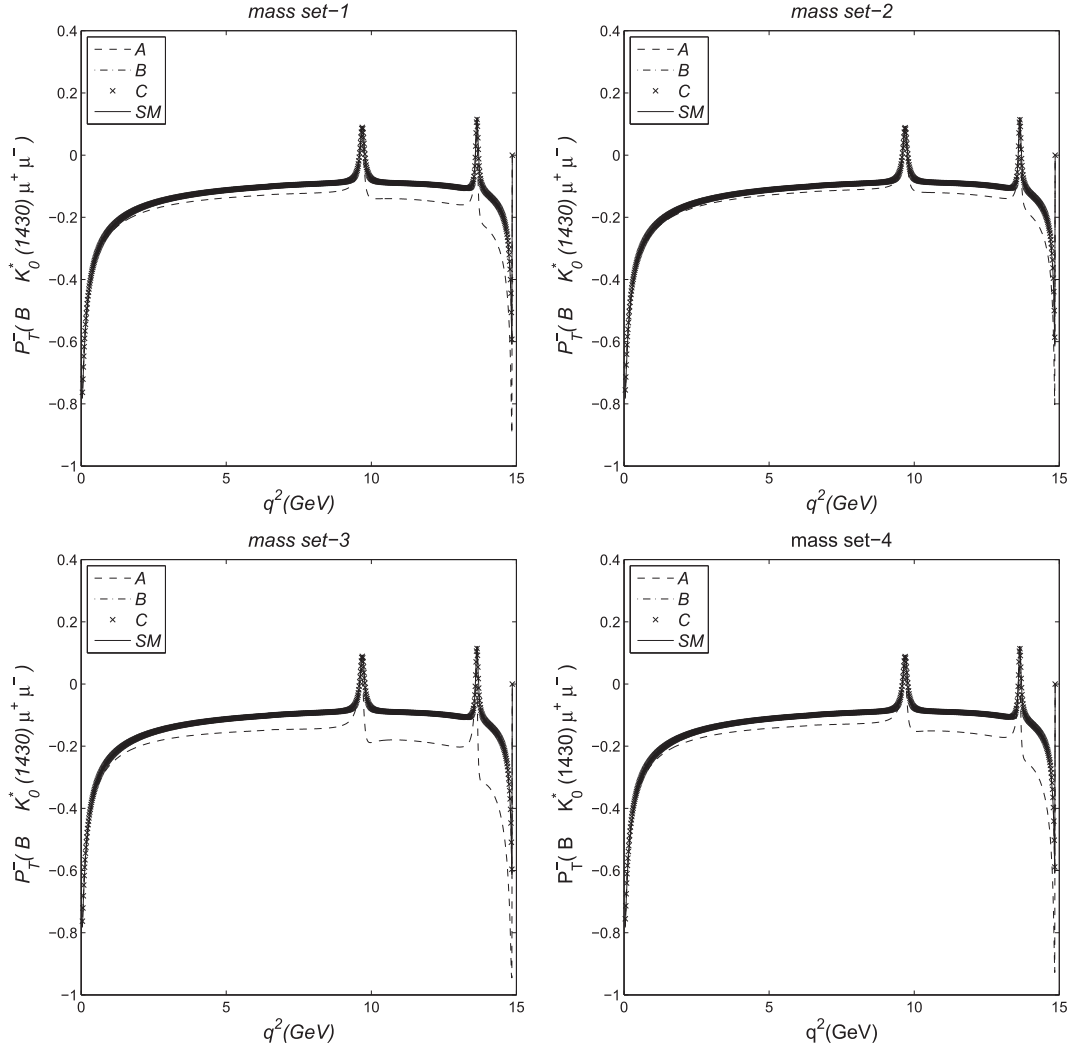


FIG. 5. The dependence of the \mathcal{P}_T^- polarization on q^2 and the three typical cases of the 2HDM, i.e., cases A, B, and C, and the SM for the μ channel of $\bar{B} \rightarrow \bar{K}_0^*$ transition for mass sets 1, 2, 3, and 4.

$|\lambda_{tt}\lambda_{bb}|$, the deviation from the SM value is increased. Also, this asymmetry is quite sensitive to the variation of the mass of H^\pm ; this happens due to the reduction of the mass of H^\pm such that the deviations from the SM value in mass sets 2 and 4 are more than those in mass sets 1 and 3. By combining the above analyses, it is understood that the most deviations from the SM prediction occur in case C of mass sets 2 and 4. Next to $q^2 = m_\psi^2$, in the aforementioned case and mass sets, deviations around $+0.016$ are possible as compared to the zero expectation of the SM. In addition, it is found out through the corresponding Tables V and VI that the values of averages show ignorable sensitivities to the presence of new Higgs bosons.

- (vi) Analysis of \mathcal{P}_L^\mp asymmetries for $\bar{B} \rightarrow \bar{K}_0^*\tau^+\tau^-$ decay: The relevant plots in Fig. 8 show that this

asymmetry is quite sensitive to the variation of the parameters λ_{tt} and λ_{bb} . For example, by decreasing the magnitude of $|\lambda_{tt}\lambda_{bb}|$, the deviation from the SM value is increased. Also, this asymmetry is quite sensitive to the variation of the masses of H^0 and H^\pm ; this happens due to the decrease of the mass of H^0 and the increase of the mass of H^\pm such that the deviations from the SM value in mass sets 3 and 4 are more than those in mass sets 1 and 2. By gathering the above analyses, it is understood that the most deviation from the SM prediction occurs in case A of mass set 3. Whereas the SM prediction is zero at $q^2 = (m_B - m_{K_0^*})^2$, a deviation around $+0.7$ is possible at that point. Besides, it is found out through the corresponding tables that a deviation around -4.9 times of that of SM arises in case A of mass set 3 at most. Also, it is clear from Eq. (38)

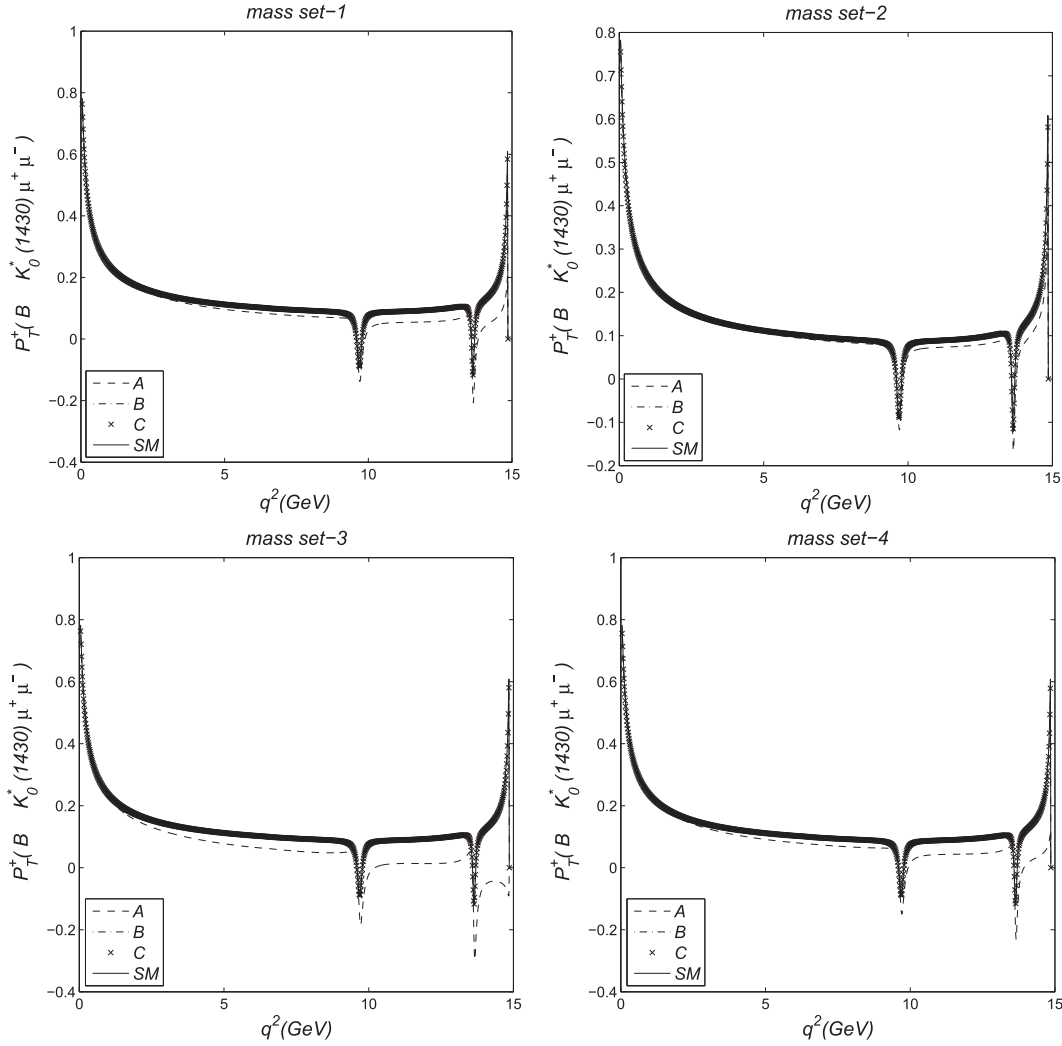


FIG. 6. The dependence of the \mathcal{P}_T^+ polarization on q^2 and the three typical cases of the 2HDM, i.e., cases A, B, and C, and the SM for the μ channel of $\bar{B} \rightarrow \bar{K}_0^* \mu^+ \mu^-$ transition for mass sets 1, 2, 3, and 4.

while by ignoring the signs of \mathcal{P}_L^- and \mathcal{P}_L^+ in the SM the magnitudes of them are the same ($\mathcal{P}_L^+ = -\mathcal{P}_L^-$ in the SM), those asymmetries do not have any symmetrical relationship with each other in the 2HDM. Nevertheless, it is evident from the corresponding Figs. 8 and 9 and tables that in cases B and C to a large extent $\mathcal{P}_L^+ = -\mathcal{P}_L^-$. The maximum deviations of \mathcal{P}_L^+ relative to the SM predictions which are observed in the respective diagrams and tables take place in case A of mass set 3 and are around +0.7 as compared to the SM expectation of zero asymmetry at $q^2 = (m_B - m_{K_0^*})^2$ and +6.6 times the calculated SM prediction for the related averages.

(vii) Analysis of \mathcal{P}_N^\mp asymmetries for $\bar{B} \rightarrow \bar{K}_0^* \tau^+ \tau^-$ decay: It is clear from Figs. 8 and 10 that the asymmetries \mathcal{P}_N^- and \mathcal{P}_L^- show the same sensitivities

to the variations of mass sets and cases. For instance, in these asymmetries, by reducing the magnitude of $|\lambda_{tt}\lambda_{bb}|$ or the mass of H^0 and enhancing the mass of H^\pm , the deviations from the SM predictions increase. According to this, the largest deviation of \mathcal{P}_N^- from the SM prediction arises in case A of mass set 3. Next to $q^2 = m_{\psi'}^2$ in the aforementioned case and mass set, a deviation around -0.04 compared to the zero prediction of the SM is possible for \mathcal{P}_N^- . In addition, it is obvious through the respective tables that the most deviation of $\langle \mathcal{P}_N^- \rangle$ from the calculated SM value is -0.024 , which happens in case A of mass set 3. Moreover, it is clear from Eq. (39) that in the SM $\mathcal{P}_N^+ = \mathcal{P}_N^- = 0$ and in the 2HDM $\mathcal{P}_N^+ = -\mathcal{P}_N^-$.

(viii) Analysis of \mathcal{P}_T^\mp asymmetries for $\bar{B} \rightarrow \bar{K}_0^* \tau^+ \tau^-$ decay: Since our analyses for all the aforementioned

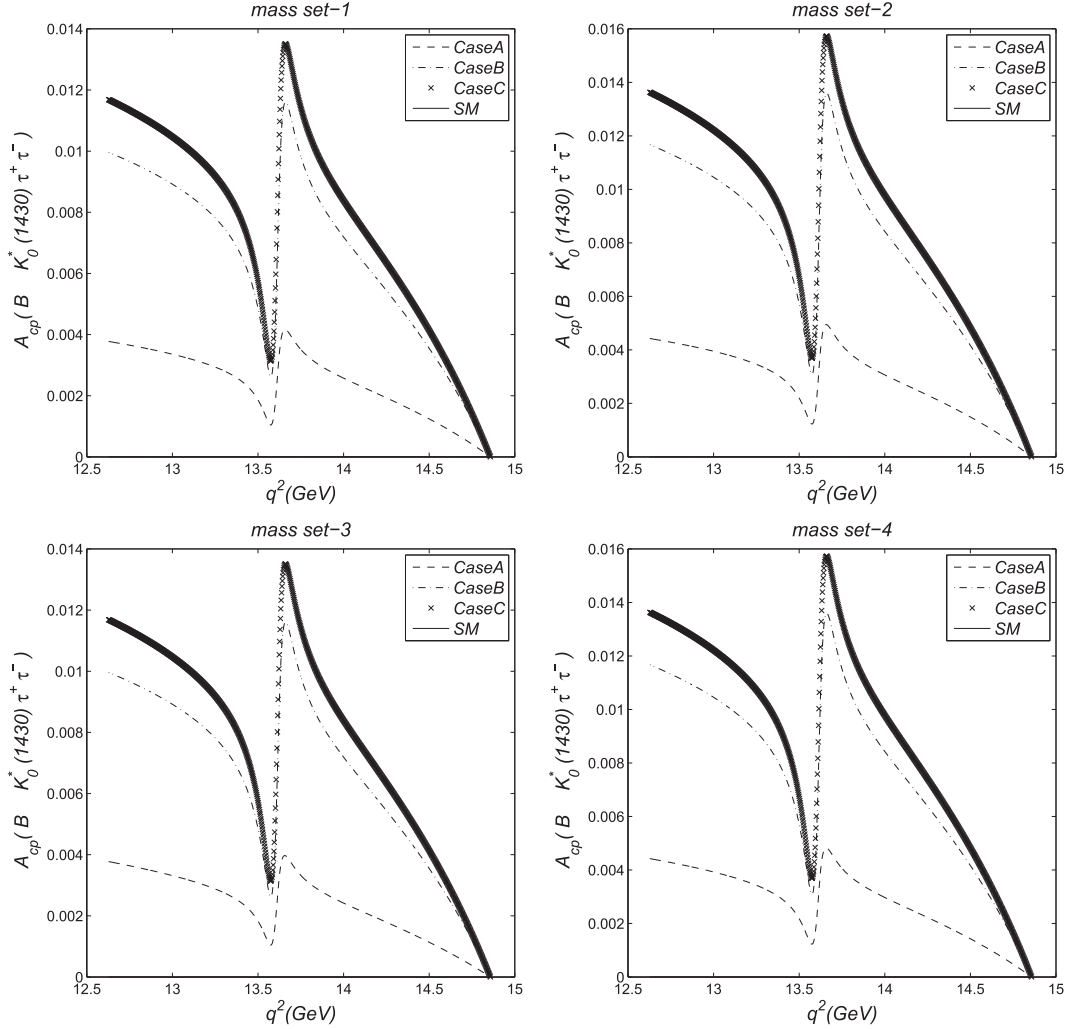


FIG. 7. The dependence of the \mathcal{A}_{CP} polarization on q^2 and the three typical cases of the 2HDM, i.e., cases A, B, and C, and the SM for the τ channel of $\bar{B} \rightarrow \bar{K}_0^* \tau^+ \tau^-$ transition for mass sets 1, 2, 3, and 4.

mass sets show that $\mathcal{P}_{T2HDM}^- = \mathcal{P}_{TSM}^-$ in all cases and $\mathcal{P}_{T2HDM}^+ = \mathcal{P}_{TSM}^+$ in cases B and C, we have only presented the plots of mass set 3 for \mathcal{P}_T^\mp in Fig. 11. In this mass set, the most deviation from the SM value for \mathcal{P}_T^+ arises somehow in case A of the range $m_\psi^2 < q^2 < (m_B - m_{K_0^*})^2$, and a discrepancy of about -25% SM is seen. Also, it is clear from the corresponding tables that the largest deviation from the calculated SM anticipation for $\langle \mathcal{P}_T^+ \rangle$ is -15% SM and occurs in the mentioned case and mass set. Moreover, it is clear from Eq. (40) that $\mathcal{P}_T^+ = -\mathcal{P}_T^-$ in the SM.

Finally, let us see briefly whether the lepton polarization asymmetries are visitable or not. To measure an asymmetry $\langle \mathcal{A} \rangle$ of the decay with branching ratio \mathcal{B} at the $n\sigma$ level in experiment, the required number of events (i.e., the number of $B\bar{B}$) is given by the relation

$$N = \frac{n^2}{\mathcal{B}s_1s_2\langle \mathcal{A} \rangle^2},$$

where s_1 and s_2 are the efficiencies of the leptons. The values of the efficiencies of the τ leptons differ from 50% to 90% for their different decay modes [31], and the error in τ -lepton polarization is nearly 10%–15% [32]. So, the error in the measurements of the τ -lepton asymmetries is estimated to be about 20%–30%, and the error in obtaining the number of events is about 50%.

According to the above expression for N , in order to measure the single lepton polarization asymmetries in the μ and τ channels at 3σ level, the lowest limit of the required number of events is given by (the efficiency of the τ lepton is considered 0.5)

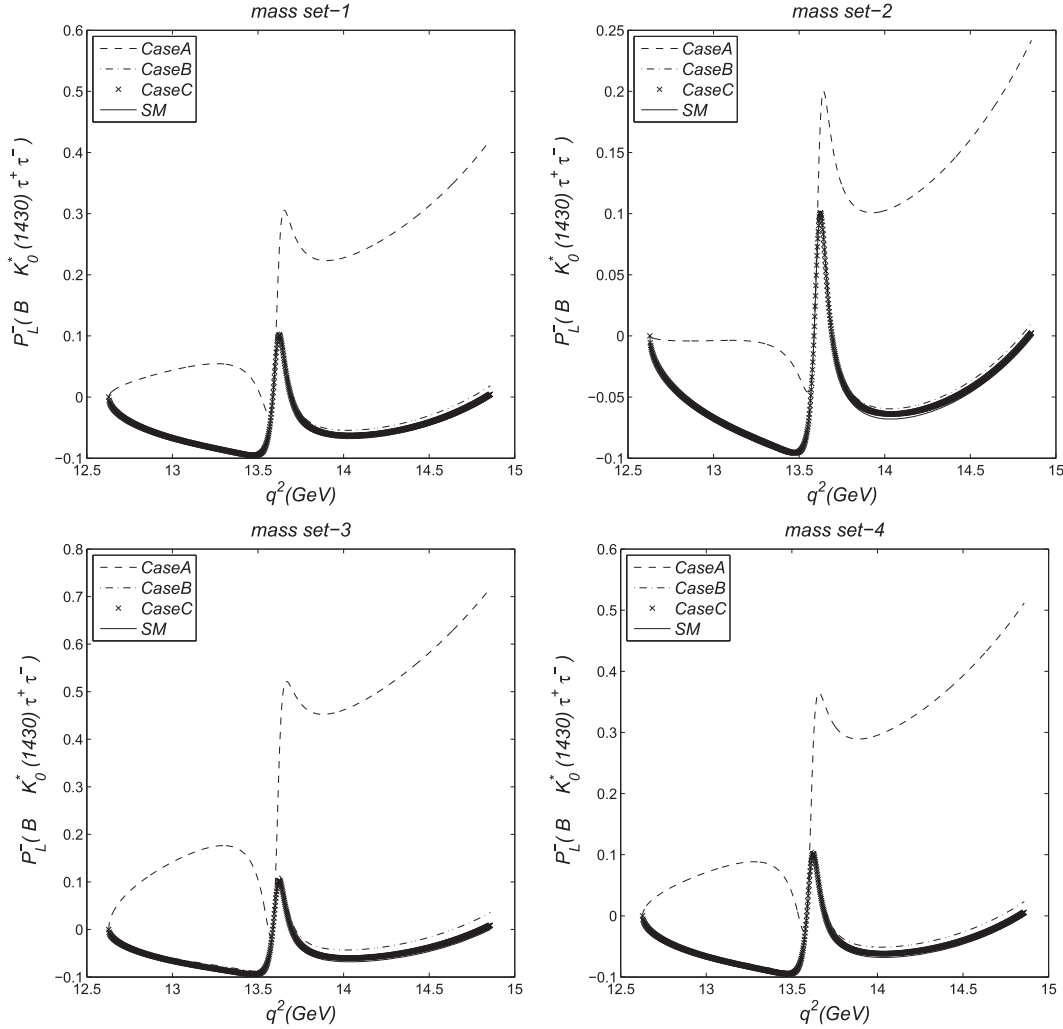


FIG. 8. The dependence of the \mathcal{P}_L^- polarization on q^2 and the three typical cases of the 2HDM, i.e., cases A, B, and C, and the SM for the τ channel of $\bar{B} \rightarrow \bar{K}_0^*(1430)\tau^+\tau^-$ transition for mass sets 1, 2, 3, and 4.

(i) for $\bar{B} \rightarrow \bar{K}_0^*(1430)\mu^+\mu^-$ decay

$$N \sim \begin{cases} 10^{24} & (\text{for } \langle \mathcal{A}_{CP} \rangle), \\ 10^7 & (\text{for } \langle \mathcal{P}_L^- \rangle, \langle \mathcal{P}_L^+ \rangle), \\ 10^8 & (\text{for } \langle \mathcal{P}_T^- \rangle, \langle \mathcal{P}_T^+ \rangle), \\ 10^{12} & (\text{for } \langle \mathcal{P}_N^- \rangle, \langle \mathcal{P}_N^+ \rangle), \end{cases}$$

(ii) for $\bar{B} \rightarrow \bar{K}_0^*(1430)\tau^+\tau^-$ decay

$$N \sim \begin{cases} 10^{27} & (\text{for } \langle \mathcal{A}_{CP} \rangle), \\ 10^{10} & (\text{for } \langle \mathcal{P}_L^- \rangle, \langle \mathcal{P}_L^+ \rangle), \\ 10^{10} & (\text{for } \langle \mathcal{P}_T^- \rangle, \langle \mathcal{P}_T^+ \rangle), \\ 10^{13} & (\text{for } \langle \mathcal{P}_N^- \rangle, \langle \mathcal{P}_N^+ \rangle), \end{cases}$$

V. SUMMARY

In short, in this paper, by considering the theoretical and experimental uncertainties in the SM, we have presented a full analysis related to the CP -violating effects and single lepton polarization asymmetries for $\bar{B} \rightarrow \bar{K}_0^*(1430)\ell^+\ell^-$ decay in model III of the 2HDM. At the same time, we have compared the results of both the μ and τ channels to each other. Also, the minimum required number of events for measuring each asymmetry has been obtained and compared with those in LHC experiments, containing ATLAS, CMS, and LHCb, ($\sim 10^{12}$ per year) or expected to be produced at the Super-LHC experiments (supposed to be $\sim 10^{13}$ per year). In conclusion, the following results have been obtained:

(i) For the μ channel of single lepton polarization asymmetries [$\mathcal{P}_i^\mp(q^2)$, $i = L, N, T$], only the results obtained from case A differ from the SM

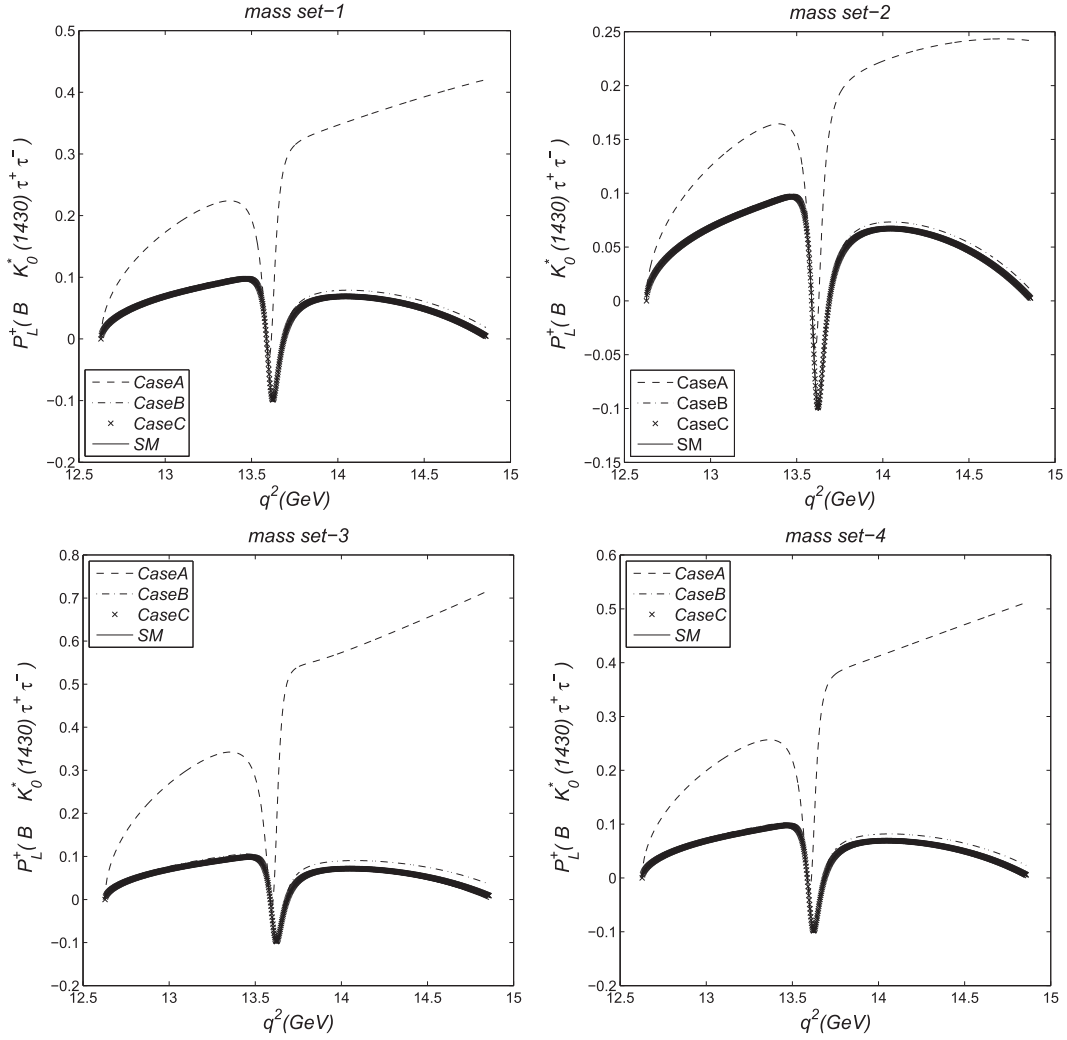


FIG. 9. The dependence of the \mathcal{P}_L^+ polarization on q^2 and the three typical cases of the 2HDM, i.e., cases A, B, and C, and the SM for the τ channel of $\bar{B} \rightarrow \bar{K}_0^*(1430)\tau^+\tau^-$ transition for mass sets 1, 2, 3, and 4.

expectations. This fact indicates that these asymmetries are quite sensitive to the reduction of $|\lambda_{tt}\lambda_{bb}|$. Also, the decrease of the mass of H^0 and simultaneously the increase of the mass of H^\pm can enhance the deviations from the SM predictions. Based on the above explanations in all single lepton polarization asymmetries, the most deviations from the SM values happen in case A of mass set 3. On the other hand, for the μ channel of CP -violating asymmetry $[\mathcal{A}_{CP}(q^2)]$, the results obtained from all cases are different from that of the SM, and somehow the biggest deviation from the SM anticipation occurs in case C. This fact indicates that this asymmetry is quite sensitive to the enhancement of $|\lambda_{tt}\lambda_{bb}|$. Also, while this asymmetry is quite insensitive to the variation of the mass of H^0 , the deviations from the SM prediction increase by decreasing the mass of H^\pm . Based on the above

explanations in CP -violating asymmetry, the most deviations from the SM value happen in case C of mass sets 2 and 4. Paying attention to the minimum required number of events for detecting each asymmetry, it is inferred that, while all single lepton polarization asymmetries are detectable at the LHC, CP -violating asymmetry is not measurable in either the LHC nor Super Large Hadron Collider (SLHC).

- (ii) For the τ channel of $\mathcal{P}_T^-(q^2)$, any sensitivity to the 2HDM parameters is not seen, and for the τ channel of other single lepton polarization asymmetries $[\mathcal{P}_T^+(q^2), \mathcal{P}_i^\mp(q^2) i = L, N]$, only the results obtained from case A differ from the SM expectations. This fact indicates that these asymmetries are quite sensitive to the reduction of $|\lambda_{tt}\lambda_{bb}|$. Also, the decrease of the mass of H^0 and simultaneously the increase of the mass of H^\pm can enhance the

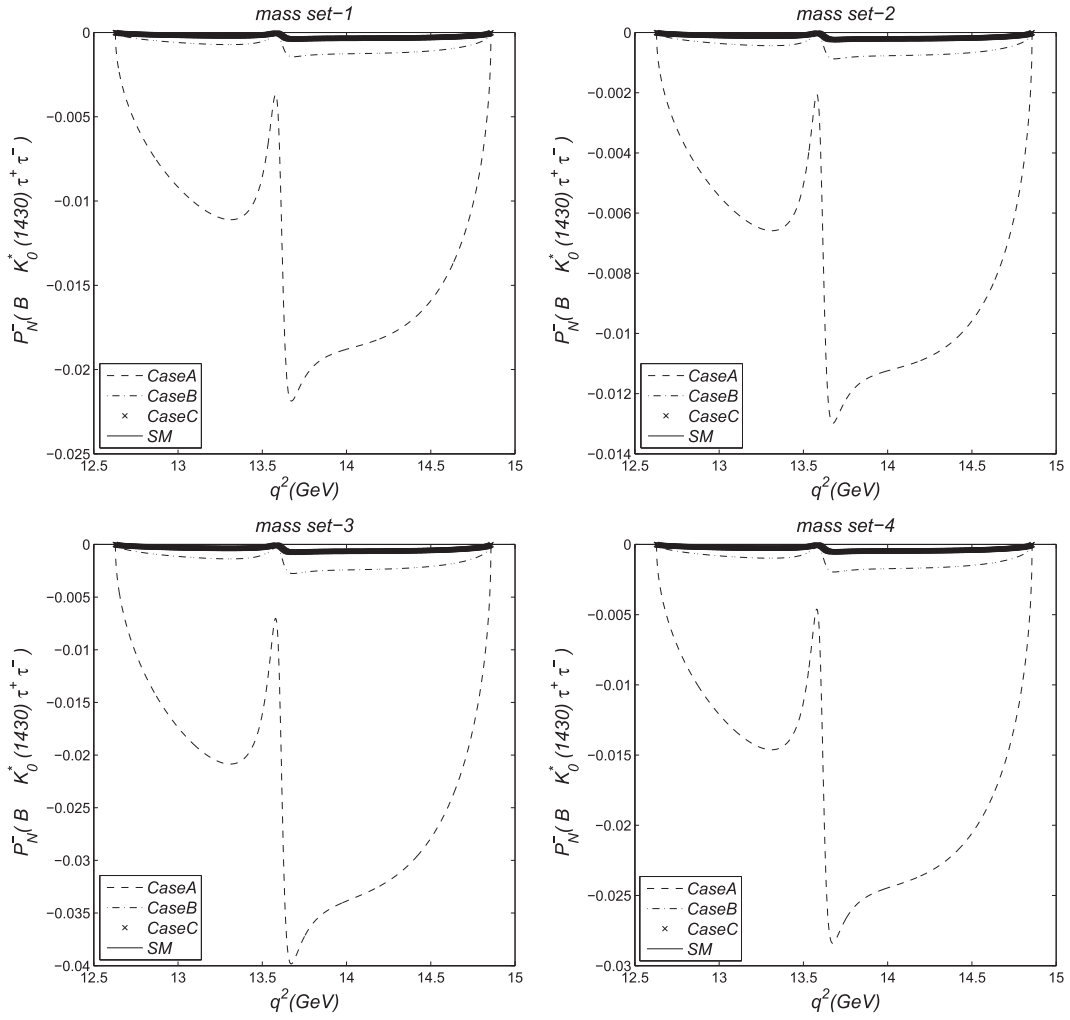


FIG. 10. The dependence of the \mathcal{P}_N^- polarization on q^2 and the three typical cases of the 2HDM, i.e., cases A, B, and C, and the SM for the τ channel of $\bar{B} \rightarrow \bar{K}_0^*$ transition for mass sets 1, 2, 3, and 4.

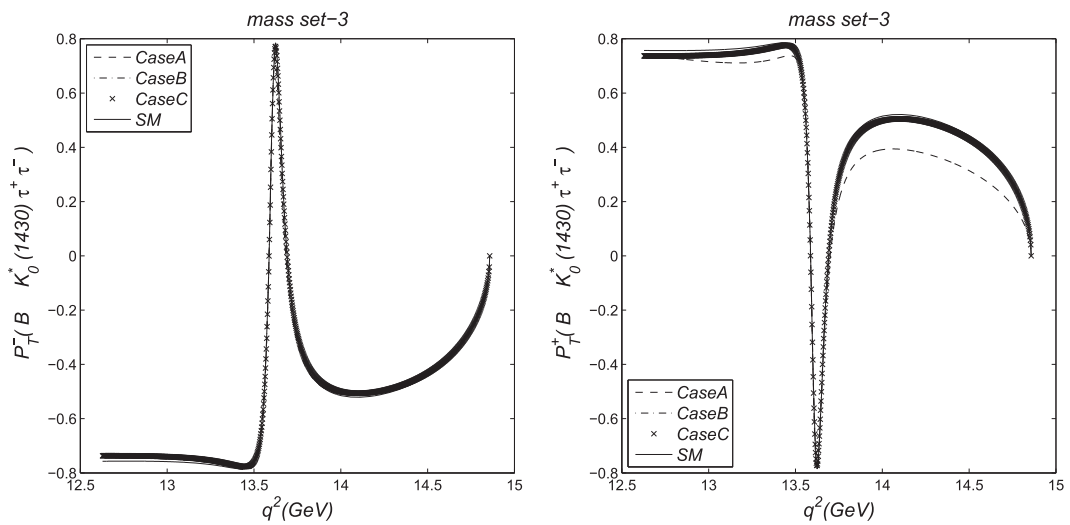


FIG. 11. The dependence of the \mathcal{P}_T^+ polarizations on q^2 and the three typical cases of the 2HDM, i.e., cases A, B, and C, and the SM for the τ channel of $\bar{B} \rightarrow \bar{K}_0^*$ transition for mass set 3.

TABLE III. The averaged CP -violation and single lepton polarization asymmetries for $\bar{B} \rightarrow \bar{K}_0^*(1430)\mu^+\mu^-$ in the SM and 2HDM for mass sets 1 and 2 of the Higgs bosons and the three cases A ($\theta = \pi/2$, $|\lambda_{tt}| = 0.03$, and $|\lambda_{bb}| = 100$), B ($\theta = \pi/2$, $|\lambda_{tt}| = 0.15$, and $|\lambda_{bb}| = 50$), and C ($\theta = \pi/2$, $|\lambda_{tt}| = 0.3$, and $|\lambda_{bb}| = 30$). The errors shown for each asymmetry are due to the theoretical and experimental uncertainties. The first ones are related to the theoretical uncertainties, and the second ones are due to experimental uncertainties. The theoretical uncertainties come from the hadronic uncertainties related to the form factors, and the experimental uncertainties originate from the mass of quarks and hadrons and Wolfenstein parameters.

		Case A	Case B	Case C	Case A	Case B	Case C
SM		(Set 1)	(Set 1)	(Set 1)	(Set 2)	(Set 2)	(Set 2)
$\langle \mathcal{A}_{CP} \rangle$	$0.000_{-0.000-0.000}^{+0.000+0.000}$	+0.001	+0.004	+0.004	+0.002	+0.004	+0.005
$\langle \mathcal{P}_L^- \rangle$	$-0.952_{-0.002-0.001}^{+0.002+0.001}$	-0.945	-0.934	-0.929	-0.945	-0.928	-0.922
$\langle \mathcal{P}_T^- \rangle$	$-0.158_{-0.012-0.002}^{+0.009+0.002}$	-0.179	-0.156	-0.154	-0.170	-0.154	-0.153
$\langle \mathcal{P}_N^- \rangle$	$0.000_{-0.000-0.000}^{+0.000+0.000}$	-0.002	-0.000	-0.000	-0.001	-0.000	-0.000
$\langle \mathcal{P}_L^+ \rangle$	$+0.952_{-0.002-0.001}^{+0.002+0.001}$	+0.950	+0.934	+0.930	+0.948	+0.929	+0.922
$\langle \mathcal{P}_T^+ \rangle$	$+0.158_{-0.012-0.002}^{+0.009+0.002}$	+0.140	+0.154	+0.154	+0.149	+0.154	+0.153
$\langle \mathcal{P}_N^+ \rangle$	$0.000_{-0.000-0.000}^{+0.000+0.000}$	+0.002	+0.000	+0.000	+0.001	+0.000	+0.000

TABLE IV. The same as Table III but for mass sets 3 and 4 of the Higgs bosons.

		Case A	Case B	Case C	Case A	Case B	Case C
SM		(Set 3)	(Set 3)	(Set 3)	(Set 4)	(Set 4)	(Set 4)
$\langle \mathcal{A}_{CP} \rangle$	$0.000_{-0.000-0.000}^{+0.000+0.000}$	+0.001	+0.004	+0.004	+0.002	+0.004	+0.005
$\langle \mathcal{P}_L^- \rangle$	$-0.952_{-0.002-0.001}^{+0.002+0.001}$	-0.942	-0.934	-0.929	-0.943	-0.928	-0.922
$\langle \mathcal{P}_T^- \rangle$	$-0.158_{-0.012-0.002}^{+0.009+0.002}$	-0.196	-0.156	-0.155	-0.183	-0.155	-0.153
$\langle \mathcal{P}_N^- \rangle$	$0.000_{-0.000-0.000}^{+0.000+0.000}$	-0.004	-0.000	-0.000	-0.003	-0.000	-0.000
$\langle \mathcal{P}_L^+ \rangle$	$+0.952_{-0.002-0.001}^{+0.002+0.001}$	+0.952	+0.935	+0.930	+0.950	+0.929	+0.922
$\langle \mathcal{P}_T^+ \rangle$	$+0.158_{-0.012-0.002}^{+0.009+0.002}$	+0.123	+0.154	+0.154	+0.136	+0.153	+0.153
$\langle \mathcal{P}_N^+ \rangle$	$0.000_{-0.000-0.000}^{+0.000+0.000}$	+0.004	+0.000	+0.000	+0.003	+0.000	+0.000

TABLE V. The same as Table III except for $\bar{B} \rightarrow \bar{K}_0^*(1430)\tau^+\tau^-$.

		Case A	Case B	Case C	Case A	Case B	Case C
SM		(Set 1)	(Set 1)	(Set 1)	(Set 2)	(Set 2)	(Set 2)
$\langle \mathcal{A}_{CP} \rangle$	$0.000_{-0.000-0.000}^{+0.000+0.000}$	+0.001	+0.003	+0.003	+0.001	+0.003	+0.004
$\langle \mathcal{P}_L^- \rangle$	$-0.066_{-0.077-0.013}^{+0.030+0.011}$	+0.147	-0.056	-0.066	+0.057	-0.060	-0.063
$\langle \mathcal{P}_T^- \rangle$	$-0.628_{-0.127-0.017}^{+0.123+0.010}$	-0.619	-0.619	-0.612	-0.616	-0.617	-0.609
$\langle \mathcal{P}_N^- \rangle$	$0.000_{-0.000-0.000}^{+0.000+0.000}$	-0.013	-0.001	-0.000	-0.008	-0.001	-0.000
$\langle \mathcal{P}_L^+ \rangle$	$+0.066_{-0.077-0.013}^{+0.030+0.011}$	+0.266	+0.073	+0.066	+0.176	+0.069	+0.065
$\langle \mathcal{P}_T^+ \rangle$	$+0.628_{-0.127-0.017}^{+0.123+0.010}$	+0.579	+0.617	+0.612	+0.593	+0.616	+0.609
$\langle \mathcal{P}_N^+ \rangle$	$0.000_{-0.000-0.000}^{+0.000+0.000}$	+0.013	+0.001	+0.000	+0.008	+0.001	+0.000

TABLE VI. The same as Table V but for mass sets 3 and 4 of the Higgs bosons.

SM		Case A (Set 3)	Case B (Set 3)	Case C (Set 3)	Case A (Set 4)	Case B (Set 4)	Case C (Set 4)
$\langle \mathcal{A}_{CP} \rangle$	$0.000_{-0.000-0.000}^{+0.000+0.000}$	+0.001	+0.003	+0.003	+0.001	+0.003	+0.004
$\langle \mathcal{P}_L^- \rangle$	$-0.066_{-0.077-0.013}^{+0.030+0.011}$	+0.322	-0.049	-0.060	+0.197	-0.054	-0.061
$\langle \mathcal{P}_T^- \rangle$	$-0.628_{-0.127-0.017}^{+0.123+0.010}$	-0.611	-0.620	-0.613	-0.617	-0.617	-0.609
$\langle \mathcal{P}_N^- \rangle$	$0.000_{-0.000-0.000}^{+0.000+0.000}$	-0.024	-0.002	-0.000	-0.017	-0.001	-0.000
$\langle \mathcal{P}_L^+ \rangle$	$+0.066_{-0.077-0.013}^{+0.030+0.011}$	+0.436	+0.081	+0.068	+0.314	+0.075	+0.067
$\langle \mathcal{P}_T^+ \rangle$	$+0.628_{-0.127-0.017}^{+0.123+0.010}$	+0.537	+0.617	+0.612	+0.567	+0.615	+0.609
$\langle \mathcal{P}_N^+ \rangle$	$0.000_{-0.000-0.000}^{+0.000+0.000}$	+0.024	+0.002	+0.000	+0.017	+0.001	+0.000

deviations from the SM predictions. Based on the above explanations, in all single lepton polarization asymmetries except \mathcal{P}_T^- , the most deviations from the SM values happen in case A of mass set 3. On the other hand, for the τ channel of CP -violating asymmetry [$\mathcal{A}_{CP}(q^2)$], the results obtained from all cases are different from that of the SM, and somehow the biggest deviation from the SM anticipation occurs in case C. This fact indicates that this asymmetry is quite sensitive to the enhancement of $|\lambda_{tt}\lambda_{bb}|$. Also, while this asymmetry is quite insensitive to the variation of the mass of H^0 , the deviations from the SM prediction increase by decreasing the mass of H^\pm . Paying attention to the minimum required number of events for detecting each asymmetry, it is inferred that \mathcal{P}_L^\mp and \mathcal{P}_T^\mp are detectable at the LHC, \mathcal{P}_N^\mp is measurable at the SLHC, and CP -violating asymmetry is not detectable in the LHC nor SLHC.

- (iii) For the μ channel, in $\langle \mathcal{P}_L^\mp \rangle$, the results of cases B and C for all mass sets do not lie between the limits of the SM prediction. The maximum deviations of these asymmetries from the calculated values of the SM happen in case C of mass sets 2 and 4 and are -3.2% SM. In $\langle \mathcal{P}_N^\mp \rangle$, the results of case A for all mass sets do not lie between the limits of calculated SM prediction. The most deviations from the zero predictions of the SM happen in case A of mass set 3 and are ∓ 0.004 . In $\langle \mathcal{P}_T^\mp \rangle$, the results of case A for mass sets 1, 3, and 4 do not lie between the limits of the SM prediction. The most deviations of $\langle \mathcal{P}_T^- \rangle$ and $\langle \mathcal{P}_T^+ \rangle$ from the calculated values of the SM happen in case A of mass set 3 and are $+24\%$ SM and -22% SM, respectively. In $\langle \mathcal{A}_{CP} \rangle$, the results of all cases for all mass sets do not lie between the limits of the SM prediction. The most deviations from the zero prediction of the SM happen in case C of mass sets 2 and 4 and are $+0.005$.

- (iv) For the τ channel, in $\langle \mathcal{P}_L^\mp \rangle$, the results of case A for all mass sets do not lie between the limits of the SM prediction. The most deviations of $\langle \mathcal{P}_L^- \rangle$ and $\langle \mathcal{P}_L^+ \rangle$ from the obtained values in the SM happen in case A of mass set 3 and are -4.9 times that of the SM and $+6.6$ times that of the SM, respectively. In $\langle \mathcal{P}_N^\mp \rangle$, the results of cases A and B for all mass sets do not lie between the limits of the SM prediction. The most deviations from the zero predictions of the SM happen in case A of mass set 3 and are ∓ 0.024 . In $\langle \mathcal{P}_T^\mp \rangle$, the results of all cases and mass sets lie between the limits of SM predictions although the most deviation of $\langle \mathcal{P}_T^+ \rangle$ from the calculated value of SM is -15% SM. In $\langle \mathcal{A}_{CP} \rangle$, the results of all cases and mass sets do not lie between the limits of the SM prediction. The most deviations from the zero prediction of the SM happen in case C of mass sets 2 and 4 and are $+0.004$.
- (v) By comparing the asymmetries of two channels, it is understood that, first, the $\langle \mathcal{A}_{CP} \rangle$ and $\langle \mathcal{P}_T^\mp \rangle$ of the μ channel are more sensitive to the presence of new Higgs bosons than those of the τ channel and, second, the $\langle \mathcal{P}_L^\mp \rangle$ and $\langle \mathcal{P}_N^\mp \rangle$ of the τ channel show more dependency on the existence of new Higgs bosons than those of the μ channel.

Finally, it is worth mentioning that, although the muon polarization is measured for stationary muons, such experiments will be very hard to perform in the near future. The tau polarization can be studied by investigating the decay products of tau. The measurement of tau polarization in this respect is easier than the polarization of the muon.

ACKNOWLEDGMENTS

The authors would like to thank V. Bashiry for his useful discussions. Support of Research Council of Shiraz University is gratefully acknowledged.

- [1] ATLAS Collaboration, *Phys. Lett. B* **716**, 1 (2012).
- [2] CMS Collaboration, *Phys. Lett. B* **716**, 30 (2012).
- [3] CMS Collaboration, *J. High Energy Phys.* **06** (2013) 081.
- [4] T. M. Aliev and M. Savci, *Phys. Rev. D* **60**, 014005 (1999).
- [5] D. Bowser-Chao, K. Cheung, and W. Y. Keung, *Phys. Rev. D* **59**, 115006 (1999).
- [6] D. Atwood, L. Reina, and A. Soni, *Phys. Rev. D* **55**, 3156 (1997).
- [7] C. S. Huang and S. H. Zhu, *Phys. Rev. D* **68**, 114020 (2003).
- [8] Y. B. Dai, C. S. Huang, J. T. Li, and W. J. Li, *Phys. Rev. D* **67**, 096007 (2003).
- [9] B. Aubert *et al.* (BABAR Collaboration), *Phys. Rev. Lett.* **93**, 081802 (2004).
- [10] M. I. Iwasaki *et al.* (BELLE Collaboration), *Phys. Rev. D* **72**, 092005 (2005).
- [11] K. Abe *et al.* (BELLE Collaboration), *Phys. Rev. Lett.* **88**, 021801 (2001).
- [12] B. Aubert *et al.* (BABAR Collaboration), *Phys. Rev. Lett.* **91**, 221802 (2003).
- [13] A. Ishikawa *et al.* (BELLE Collaboration), *Phys. Rev. Lett.* **91**, 261601 (2003).
- [14] P. Colangelo, F. De Fazio, P. Santorelli, and E. Scrimieri, *Phys. Rev. D* **53**, 3672 (1996); **57**, 3186(E) (1998); A. Ali, P. Ball, L. T. Handoko, and G. Hiller, *Phys. Rev. D* **61**, 074024 (2000); A. Ali, E. Lunghi, C. Greub, and G. Hiller, *Phys. Rev. D* **66**, 034002 (2002).
- [15] T. M. Aliev, H. Koru, A. Ozpineci, and M. Savc, *Phys. Lett. B* **400**, 194 (1997); T. M. Aliev, A. Ozpineci, and M. Savc, *Phys. Rev. D* **56**, 4260 (1997); D. Melikhov, N. Nikitin, and S. Simula, *Phys. Rev. D* **57**, 6814 (1998).
- [16] G. Burdman, *Phys. Rev. D* **52**, 6400 (1995); J. L. Hewett and J. D. Wells, *Phys. Rev. D* **55**, 5549 (1997); C. H. Chen and C. Q. Geng, *Phys. Rev. D* **63**, 114025 (2001).
- [17] S. Rai Choudhury, A. S. Cornell, G. C. Joshi, and B. H. J. McKellar, *Phys. Rev. D* **74**, 054031 (2006).
- [18] H. Y. Cheng, C. K. Chua, and C. W. Huang, *Phys. Rev. D* **69**, 074025 (2004).
- [19] H. Y. Cheng and C. K. Chua, *Phys. Rev. D* **69**, 094007 (2004).
- [20] C. H. Chen, C. Q. Geng, C. C. Lih, and C. C. Liu, *Phys. Rev. D* **75**, 074010 (2007).
- [21] T. M. Aliev, K. Azizi, and M. Savci, *Phys. Rev. D* **76**, 074017 (2007).
- [22] K. C. Yang, *Phys. Lett. B* **695**, 444 (2011).
- [23] A. J. Buras and M. Munz, *Phys. Rev. D* **52**, 186 (1995).
- [24] M. Kobayashi and M. Maskawa, *Prog. Theor. Phys.* **49**, 652 (1973).
- [25] T. P. Cheng and M. Sher, *Phys. Rev. D* **35**, 3484 (1987); **44**, 1461 (1991).
- [26] B. Grinstein, M. J. Savage, and M. B. Wise, *Nucl. Phys.* **B319**, 271 (1989).
- [27] Y. B. Dai, C. S. Huang, and H. W. Huang, *Phys. Lett. B* **390**, 257 (1997).
- [28] F. Kruger and L. M. Sehgal, *Phys. Lett. B* **380**, 199 (1996).
- [29] V. Bashiry M. Bayar and K. Azizi, *Mod. Phys. Lett. A* **26**, 901 (2011).
- [30] T. M. Aliev, M. K. Cakmak, A. Ozpineci, and M. Savci, *Phys. Rev. D* **64**, 055007 (2001).
- [31] G. Abbiendi *et al.* (OPAL Collaboration), *Phys. Lett. B* **492**, 23 (2000).
- [32] A. Rouge, *Z. Phys. C* **48**, 75 (1990); Proceedings of the Workshop on τ Lepton Physics, Orsay, France, 1990 (unpublished).